

# 14 |

## Renormalization of gauge fields

In the previous chapter we introduced the Lagrangian that must be used in the calculation of Feynman diagrams with closed loops for generic gauge theories. In this chapter we turn to the calculation of one-loop diagrams in a nonabelian gauge theory coupled to fermions. We shall evaluate the infinite contributions of the diagrams and show how they can be absorbed in the allowed counterterms, thus establishing the renormalizability of the theory at the one-loop level.

The calculations are performed in a class of Lorentz gauges and may be regarded as the nonabelian analogue of the calculations performed for the abelian gauge theory (i.e. quantum electrodynamics) in chapters 9 and 10; we will in fact make use of the results recorded in these chapters whenever possible. The calculations will be for a general gauge group. The case of  $SU(3)$  is particularly relevant, as this is the gauge group that underlies quantum chromodynamics, the gauge theory of the strong interactions. This theory will be discussed in later chapters.

We shall start by recalling some of the main ingredients and derive some group-theoretical results needed for the subsequent calculations. Then we turn to a discussion of the renormalization and derive the counterterm Lagrangian. We demonstrate that all the ultraviolet infinities that we determine subsequently can be absorbed by these counterterms, and thereby establish the one-loop renormalizability. Then we present the explicit calculation of the infinite graphs, first for the fermions (as they follow mostly from previous results) and then for the pure gauge theory. We demonstrate how ultraviolet and infrared divergences can be disentangled in dimensional regularization, and determine all the ultraviolet one-loop divergences. Readers who are not interested in these somewhat cumbersome calculations may prefer to ignore part of this chapter and proceed to the next chapter where we discuss the phenomenon of asymptotic freedom, whose existence can be inferred from the one-loop results evaluated in this chapter, and the consequences of having different mass scales in a quantum field theory.

### 14.1. Preliminaries

The relevant Lagrangians for the gauge fields and the gauge-fixing terms in the Lorentz gauge were already given in section 13.5. The interactions with the

gauge fields are determined by the generators and the structure constants,  $t_a$  and  $f_{ab}{}^c$ . We restrict ourselves to compact simple gauge groups (for a precise definition of these concepts, see appendix C). In that case the gauge-field indices  $a, b, \dots$  can be freely raised and lowered and  $f_{abc}$  is antisymmetric in all three indices. As explained in section 12.3, compact gauge groups are required in order that the kinetic terms for each of the gauge fields in the Lagrangian are nonvanishing and of equal signs. The restriction to simple groups is just for convenience and has no important consequences; compact groups can always be written as products of simple groups, i.e. groups that have no invariant subgroup, so that the corresponding gauge-field Lagrangian can be written as a sum of the gauge-field Lagrangians for each of the invariant subgroups. The gauge fields interact with matter fields such that the generators  $t_a$  associated with different subgroups commute.

We recall that the gauge group generators satisfy the commutation relations

$$[t_a, t_b] = f_{ab}{}^c t_c. \quad (14.1)$$

In the *adjoint* representation associated with the gauge fields the generators are the structure constants (more precisely,  $(t_a)_{bc} = -f_{abc}$ ). Hence in this representation (14.1) takes the form of the Jacobi identity

$$f_{ab}{}^e f_{ec}{}^d + f_{bc}{}^e f_{ea}{}^d + f_{ca}{}^e f_{eb}{}^d = 0. \quad (14.2)$$

For compact simple groups, one can show that the generators and structure constants must satisfy the relation

$$t_a t_a = -C_2(R) \mathbf{I}, \quad \text{Tr}(t_a t_b) = -C_2(R) \frac{\dim R}{\dim G} \delta_{ab}, \quad (14.3)$$

where the matrices  $t_a$  refer to a single *irreducible* representation, and the coefficient<sup>1</sup>  $C_2(R)$  depends on the representation  $R$ . For compact groups,  $C_2(R)$  is always positive (or zero when the representation is trivial). In this section we are dealing with only two representations: the adjoint one for the gauge fields and another one corresponding to the fermions. The Casimir constant for the adjoint representation shall be denoted by  $C_2(G)$ , so that (14.3) takes the form

$$f_{acd} f_{bcd} = C_2(G) \delta_{ab}. \quad (14.4)$$

However, neither the structure constants nor the generators  $t_a$  are uniquely determined by (14.3), as one can still rescale all the generators uniformly (in the Lagrangian this rescaling can be absorbed into the coupling constant). To fix the overall normalization of the generators, it suffices to impose a condition

---

<sup>1</sup>These coefficients are related to the so-called quadratic Casimir invariants (see, e.g. appendix C).

on the generators in some given representation. In this context this is done by imposing, usually for some simple representation,

$$\text{Tr}(t_a t_b) = -\frac{1}{2} \delta_{ab}. \quad (14.5)$$

This fixes  $C_2(R)$  to be equal to

$$C_2(R) = \frac{1}{2} \frac{\dim G}{\dim R}. \quad (14.6)$$

For instance, for  $\text{SU}(N)$  and  $\text{SO}(N)$  the normalization (14.5) is usually imposed on the defining  $N$ -dimensional representations of the group. In that case one finds ( $N \geq 2$ )

$$C_2(N) = \begin{cases} \frac{N^2 - 1}{2N} & \text{for } \text{SU}(N), \\ \frac{N - 1}{4} & \text{for } \text{SO}(N) \end{cases}$$

since the dimensions of  $\text{SU}(N)$  and  $\text{SO}(N)$  equal  $N^2 - 1$  and  $\frac{1}{2}N(N - 1)$ , respectively. The corresponding values of  $C_2(G)$  are

$$C_2(G) = \begin{cases} N & \text{for } \text{SU}(N), \\ \frac{1}{2}(N - 2) & \text{for } \text{SO}(N). \end{cases} \quad (14.7)$$

For arbitrary groups the determination of these constants requires more detailed knowledge of the structure of the group. However, for  $\text{SU}(N)$  and  $\text{SO}(N)$  these results can be derived from relatively simple algebraic manipulations (see problem 14.1).

In the calculations that follow, one does not need explicit knowledge of the normalization conventions and the values for the coefficients  $C_2$ . The results will always be expressed in terms of  $C_2(G)$  and  $C_2(R)$  and when one is interested in a certain gauge group one simply substitutes the appropriate values for  $C_2$ . In order to express the various results in terms of these constants we need a number of simple relations; we evaluate four of them here, using (14.1- 14.4),

$$\begin{aligned} f_{abc} t_b t_c &= \frac{1}{2} f_{abc} f_{bcd} t_d = \frac{1}{2} C_2(G) t_a, \\ t_b t_a t_b &= (t_a t_b + f_{bac} t_c) t_b = -(C_2(R) - \frac{1}{2} C_2(G)) t_a, \\ \text{Tr}(t_a [t_b, t_c]) &= -C_2(R) \frac{\dim R}{\dim G} f_{abc}, \\ \text{Tr}([t_a, t_b] [t_c, t_d]) &= -C_2(R) \frac{\dim R}{\dim G} f_{abe} f_{cde}. \end{aligned} \quad (14.8)$$

The above relations hold for any representation  $R$ , so we can also write them down for the adjoint representation where  $(t_a)_{bc} = -f_{abc}$ . We then establish

the following identities,

$$\begin{aligned} f_{ade} f_{bef} f_{cfd} &= \frac{1}{2} C_2(G) f_{abc}, \\ f_{aef} \{ f_{bfg} f_{cgh} f_{dhe} - f_{bfg} f_{dgh} f_{che} \\ &\quad - f_{cfg} f_{dgh} f_{bhe} + f_{dfg} f_{cgh} f_{bhe} \} = -C_2(G) f_{abe} f_{cde}, \end{aligned} \quad (14.9)$$

Generalizations of these identities are easily derived, but are not needed in this chapter.

Before proceeding to actual calculations, we first turn to a discussion of the renormalization programme in the next section.

### 14.2. Renormalization and one-loop counterterms

In chapter 8 we gave an explicit exposition of the renormalization programme in quantum electrodynamics at the one-loop level. Here we perform the analogous exercise for the case of a nonabelian gauge theory associated with some group  $G$  and coupled to fermions in some (irreducible) representation of this group. Because the total number of fermions turns out to have important consequences for the result of our calculation, we allow an arbitrary number  $N_f$  of identical fermion multiplets. As we assume that all fermions have the same mass, this will not complicate the calculation in view of the fact that their interaction with the nonabelian gauge fields is uniquely determined by the properties of the representation.

For a renormalizable theory, the ultraviolet divergences that one encounters in the calculation of the various Feynman diagrams can consistently be absorbed into the various quantities that occur in the original Lagrangian, order by order in perturbation theory. In the theory at hand, these quantities are the gauge fields  $W_\mu^a$ , the ghost and antighost fields  $c^a$  and  $b^a$ , and the fermion fields  $\psi$ ; furthermore there are the gauge-coupling constant  $g$ , the fermion mass  $m$  and the gauge-fixing parameter  $\lambda$ . Following (9.45) we scale all these quantities by renormalization factors according to

$$\begin{aligned} W_\mu^a &\rightarrow \sqrt{Z_W} W_\mu^a, \quad \psi \rightarrow \sqrt{Z_\psi} \psi, \quad c^a \rightarrow \sqrt{Z_c} c^a, \quad b^a \rightarrow \sqrt{Z_b} b^a, \\ g &\rightarrow Z_g g, \quad m \rightarrow Z_m m, \quad \lambda \rightarrow Z_\lambda \lambda. \end{aligned} \quad (14.10)$$

In tree approximation each of the renormalization factors is equal to unity; the higher-order terms are usually infinite and generate precisely those infinite terms required to render the theory finite. These infinite terms are the so-called counterterms. They follow from substituting the redefinitions (14.10) into the Lagrangian,

$$\mathcal{L} \rightarrow \mathcal{L} + \mathcal{L}^{\text{c.t.}}. \quad (14.11)$$

Here we should already emphasize that there is no a priori reason why the counterterms are generated by multiplicative factors. In general there are additive renormalizations as well, but in this case they can be avoided. We divide the counterterms into three different terms

$$\mathcal{L}^{\text{c.t.}} = \mathcal{L}_1^{\text{c.t.}} + \mathcal{L}_2^{\text{c.t.}} + \mathcal{L}_3^{\text{c.t.}}, \quad (14.12)$$

where

$$\begin{aligned} \mathcal{L}_1^{\text{c.t.}} &= -\frac{1}{4}(Z_W - 1)(\partial_\mu W_\nu^a - \partial_\nu W_\mu^a)^2 - \frac{1}{2}\lambda^2(Z_\lambda^2 Z_W - 1)(\partial^\mu W_\mu^a)^2 \\ &\quad + g(Z_g Z_W^{3/2} - 1) f_{abc} W_\mu^a W_\nu^b \partial^\mu W^{c\nu} \\ &\quad - \frac{1}{4}g^2(Z_g^2 Z_W^2 - 1) f_{abc} f_{ade} W_\mu^b W^{d\mu} W_\nu^c W^{e\nu}, \\ \mathcal{L}_2^{\text{c.t.}} &= -(Z_p - 1) \bar{\psi} \not{\partial} \psi - m(Z_m Z_p - 1) \bar{\psi} \psi \\ &\quad + g(Z_g Z_p Z_W^{1/2} - 1) W_\mu^a \bar{\psi} \gamma^\mu t_a \psi, \\ \mathcal{L}_3^{\text{c.t.}} &= -i\lambda(Z_\lambda Z_b^{1/2} Z_c^{1/2} - 1) (\partial^\mu b^a) (\partial_\mu c^a) \\ &\quad - i\lambda g(Z_g Z_\lambda Z_W^{1/2} Z_b^{1/2} Z_c^{1/2} - 1) f_{abc} W_\mu^a (\partial^\mu b^b) c^c. \end{aligned} \quad (14.13)$$

The reader may easily verify that we have generated nine different counterterms in this way, while on the other hand we have only seven independent constants to adjust (actually, there is some arbitrariness in the choice of  $Z_b$  and  $Z_c$ , as only the product of these constants appears). Therefore, in order that the theory be renormalizable, it is important that a number of conditions between the infinities are satisfied.

The infinite terms (in one-loop approximation) will be evaluated in the subsequent sections. Here, following our exposition in chapter 8, we will simply summarize the result of these laborious calculations. In section 14.3 we calculate the divergences induced by loops that contain fermion lines. We distinguish diagrams with only external gauge fields and a closed fermion loop, and the diagrams with two external fermion lines and none or one gauge field (all other diagrams do not give rise to divergences). The diagrams with only external gauge fields are obviously proportional to the number of fermion representations. There are diagrams with two, three or four external gauge fields. In order to cancel the corresponding divergences we must add the following terms to the Lagrangian,

$$\begin{aligned} \Delta\mathcal{L} &= N_f C_2(R) \frac{\dim R}{\dim G} \frac{g^2 \mu^\epsilon}{6\pi^2} \frac{1}{\epsilon} \left\{ -\frac{1}{4}(\partial_\mu W_\nu^a - \partial_\nu W_\mu^a)^2 \right. \\ &\quad \left. + g f_{abc} W_\mu^a W_\nu^b \partial^\mu W^{c\nu} - \frac{1}{4}g^2 f_{abc} f_{ade} W_\mu^b W^{d\mu} W_\nu^c W^{e\nu} \right\}. \end{aligned} \quad (14.14)$$

The divergent contributions from graphs with external fermion lines are cancelled by the addition of the following terms,

$$\Delta\mathcal{L} = \frac{g^2\mu^\epsilon}{8\pi^2} \frac{1}{\epsilon} \left\{ -C_2(R) \lambda^{-2} \bar{\psi}\not{\partial}\psi - m C_2(R) (3 + \lambda^{-2}) \bar{\psi}\psi \right. \\ \left. + g [C_2(R) \lambda^{-2} + \frac{1}{4}C_2(G) (3 + \lambda^{-2})] W_\mu^a \bar{\psi}\gamma^\mu t_a \psi \right\}. \quad (14.15)$$

To these contributions we have to add the divergences from diagrams without any fermion lines. These are harder to calculate and discussed in sections 14.4 and 14.5. Their divergences are cancelled by the contributions from the following terms,

$$\Delta\mathcal{L} = -C_2(G) \frac{g^2\mu^\epsilon}{96\pi^2} \frac{1}{\epsilon} \left\{ -\frac{1}{4}(26 - 6\lambda^{-2}) (\partial_\mu W_\nu^a - \partial_\nu W_\mu^a)^2 \right. \\ \left. + g(17 - 9\lambda^{-2}) f_{abc} W_\mu^a W_\nu^b \partial^\mu W^{c\nu} \right. \\ \left. - \frac{1}{4}g^2 (8 - 12\lambda^{-2}) f_{abc} f_{ade} W_\mu^b W^{d\mu} W_\nu^c W^{e\nu} \right\}. \quad (14.16)$$

Finally we have the divergences coming from the ghost graphs, which are cancelled by

$$\Delta\mathcal{L} = C_2(G) \frac{g^2\mu^\epsilon}{32\pi^2} \frac{1}{\epsilon} \left\{ -i\lambda (3 - \lambda^{-2}) (\partial^\mu b^a) (\partial_\mu c^a) \right. \\ \left. + 2i\lambda^{-1} g f_{abc} W_\mu^b (\partial^\mu b^a) c^c \right\}. \quad (14.17)$$

As it turns out, the combined result from (14.14- 14.17) can be cast in the form (14.13), which confirms that the theory is renormalizable. The renormalization constants defined by (14.10) are then easily extracted and are given by

$$Z_W = 1 + \frac{g^2\mu^\epsilon}{6\pi^2} \frac{1}{\epsilon} \left\{ N_f C_2(R) \frac{\dim R}{\dim G} - \frac{1}{8}C_2(G) (13 - 3\lambda^{-2}) \right\} + O(g^4), \\ Z_\lambda = 1 - \frac{g^2\mu^\epsilon}{12\pi^2} \frac{1}{\epsilon} \left\{ N_f C_2(R) \frac{\dim R}{\dim G} - \frac{1}{8}C_2(G) (13 - 3\lambda^{-2}) \right\} + O(g^4), \\ Z_\psi = 1 + \frac{g^2\mu^\epsilon}{8\pi^2} \frac{1}{\epsilon} C_2(R) \lambda^{-2} + O(g^4), \\ Z_m = 1 + \frac{3g^2\mu^\epsilon}{8\pi^2} \frac{1}{\epsilon} C_2(R) + O(g^4), \\ Z_g = 1 - \frac{g^2\mu^\epsilon}{12\pi^2} \frac{1}{\epsilon} \left\{ N_f C_2(R) \frac{\dim R}{\dim G} - \frac{11}{4}C_2(G) \right\} + O(g^4), \\ \sqrt{Z_b Z_c} = 1 + \frac{g^2\mu^\epsilon}{12\pi^2} \frac{1}{\epsilon} \left\{ N_f C_2(R) \frac{\dim R}{\dim G} - \frac{1}{4}C_2(G) (11 - 3\lambda^{-2}) \right\} + O(g^4).$$

(14.18)

Observe that the renormalization factors associated with the mass and the coupling constant are independent of the gauge parameter  $\lambda$ . Furthermore this result agrees with that of quantum electrodynamics (cf. 9.47) in the abelian limit:  $G_2(G) = 0$  and  $N_f = C_2(R) = 1$ .

### 14.3. One-loop divergent graphs; fermions

In this section we consider all one-loop diagrams with fermions that give rise to ultraviolet divergences. Subsequently, in the next two sections, we turn to the diagrams without fermions, which are more difficult to evaluate. The first set of graphs that we consider here are those with a closed fermion loop. They are the only divergent one-loop diagrams that are proportional to the number of fermion representations  $N_f$ , as one can easily verify. Therefore they form an independent subclass of diagrams whose contributions to the counterterms should separately satisfy the restrictions imposed by renormalizability. There are three different types of graphs, depending on whether two, three or four external gauge fields are attached. These diagrams, shown in fig 14.1, are called vacuum polarization, triangle and box diagrams, for obvious reasons. Diagrams with more than four gauge fields attached to the fermion loop are finite and will thus be ignored. We should stress here that the gauge fields interact with the fermions through a vector interaction with the fermions. It is possible to incorporate also axial-vector couplings, but there is a number of subtleties in that case. We shall discuss these matters in due course. Here we note that we will still be able to make use of some of these calculations when discussing chiral couplings (combinations of vector and axial vector couplings), albeit that some caution is required.

The second set of one-loop divergent graphs with fermions have external fermion lines. As shown in fig 14.2 these are the fermion self-energy diagram and two types of vertex diagrams.

Before turning to the actual calculation we digress for a moment and turn to a brief discussion of the various infinite momentum integrals that we are about to encounter in this section as well as in the next one. Let us list the

relevant integrals,

$$\int \frac{d^n q}{i(2\pi)^n} \frac{1}{(q^2 + m^2)((q-p)^2 + m^2)} = -\frac{\mu^\epsilon}{8\pi^2} \frac{1}{\epsilon} + \text{finite terms}, \quad (14.19)$$

$$\int \frac{d^n q}{i(2\pi)^n} \frac{q_\mu}{(q^2 + m^2)((q-p)^2 + m^2)} = -\frac{\mu^\epsilon}{16\pi^2} \frac{1}{\epsilon} p_\mu + \text{finite terms}, \quad (14.20)$$

$$\int \frac{d^n q}{i(2\pi)^n} \frac{q_\mu q_\nu}{(q^2 + m^2)((q-p)^2 + m^2)((q+k)^2 + m^2)} = -\frac{\mu^\epsilon}{32\pi^2} \frac{1}{\epsilon} \eta_{\mu\nu} + \text{finite terms}, \quad (14.21)$$

$$\int \frac{d^n q}{i(2\pi)^n} \frac{q_\mu q_\nu q_\rho}{(q^2 + m^2)((q-p)^2 + m^2)((q+k)^2 + m^2)} = -\frac{\mu^\epsilon}{96\pi^2} \frac{1}{\epsilon} \left( \eta_{\mu\nu}(p-k)_\rho + \eta_{\nu\rho}(p-k)_\mu + \eta_{\rho\mu}(p-k)_\nu \right) + \text{finite terms}, \quad (14.22)$$

$$\int \frac{d^n q}{i(2\pi)^n} \frac{q_\mu q_\nu q_\rho q_\sigma}{(q^2 + m^2)^4} = -\frac{\mu^\epsilon}{192\pi^2} \frac{1}{\epsilon} \left( \eta_{\mu\nu} \eta_{\rho\sigma} + \eta_{\mu\rho} \eta_{\sigma\nu} + \eta_{\mu\sigma} \eta_{\nu\rho} \right) + \text{finite terms}. \quad (14.23)$$

The derivation of the above results follows a uniform pattern. To extract the infinite terms one makes a Taylor expansion in the external momenta. At sufficiently high order in these momenta, the integrals are finite and can be ignored. One then evaluates the infinite terms by exploiting the symmetry of the integrand, making suitable shifts in the integration variable. Needless to say these integrals can all be evaluated explicitly, including the finite terms, as we have demonstrated for certain integrals in chapter 9. The reader is advised to consult also appendix F where we listed a number of relevant  $n$ -dimensional integrals.

The first integral (14.19) was evaluated explicitly in section 9.3 (cf. 9.26). To obtain the result (14.20) we shift the integration variable  $q$  to  $q + \frac{1}{2}p$ , so that the numerator becomes  $q_\mu + \frac{1}{2}p_\mu$ . As the denominator is now symmetric under  $q \rightarrow -q$ , one may drop the  $q_\mu$  in the numerator. The result is therefore equal to  $\frac{1}{2}p_\mu$  times the integral (14.19) and this leads to the result quoted in (14.20). Expanding the third integral in terms of  $p$  and  $k$ , it turns out that the terms of higher order in these momenta are finite. To obtain the infinite terms, one may thus evaluate the integral directly for  $p = k = 0$ . This is done by symmetric integration, or, alternatively, one uses Lorentz invariance to argue that the integral must be proportional to  $\eta_{\mu\nu}$ ; this allows one to replace  $q_\mu q_\nu$  in the numerator by  $n^{-1} q^2 \eta_{\mu\nu}$ . Subsequently one changes the term  $q^2$  by  $(q^2 + m^2)$ , which only changes the integral by a finite amount, to

cancel a  $(q^2 + m^2)$  term in the denominator. Hence the infinite part of the first integral is equal to  $n^{-1}\eta_{\mu\nu}$  times the infinite part of the integral (14.19). Substituting  $n = 4$  in the residue of the  $1/\epsilon$  pole, the result (14.21) follows.

The derivation of the fourth integral follows the same steps but is a little more involved. Here the integral vanishes for  $p = k = 0$ , because the integral is then odd in  $q$ . Taylor expanding in  $p$  and  $k$  shows that only the terms linear in these momenta are infinite. From the symmetry in  $\mu, \nu, \rho$  and Lorentz invariance it then follows that the infinite part must be proportional to  $(\eta_{\mu\nu} P_\rho + \eta_{\nu\rho} P_\mu + \eta_{\rho\mu} P_\nu)$ , where  $P$  is some linear combination of  $p$  and  $k$ . As the integral changes sign under the interchange of  $p \leftrightarrow k$ , the momentum  $P$  must be proportional to  $p - k$  (to see this one must simultaneously change the integration momentum  $q$  into  $-q$ ). Having determined the tensorial structure, it remains to determine the infinite constant that multiplies it. This is done by contracting the integral with  $\eta^{\mu\nu}$ . The tensor on the right-hand side then yields  $(n + 2)(p - k)_\rho$ , while the numerator of the integrand on the left-hand side becomes equal to  $q^2 q_\rho$ . Now replace again  $q^2$  by  $(q^2 + m^2)$ , which only changes the integral by a finite amount, to cancel the factor  $(q^2 + m^2)$  in the denominator. The result is then an integral of type (14.19) and (14.20) upon an appropriate shift of the integration momentum. Substituting the result given in (14.20) and substituting  $n = 4$  in the residue of the  $1/\epsilon$  term gives the result quoted in (14.22).

Finally, the result for the integral (14.23) follows from Lorentz invariance and the symmetry in  $\mu, \nu, \rho$  and  $\sigma$ , from which one deduces that the tensorial structure of the integral must take the form indicated in (14.23). The infinite proportionality constant is then determined by contracting the integral by  $\eta^{\mu\nu} \eta^{\rho\sigma}$ , which leads to a factor  $q^4$  in the numerator of the integrand, which can be modified by adding  $m^2$  terms to cancel against similar terms in the denominator. Again this modification introduces only finite terms. On the right-hand side the contraction leads to a factor  $n(n + 2)$ . Comparing this result with the integral (14.19) then gives the above result after substituting  $n = 4$  in the residue of the  $1/\epsilon$  pole.

We are now fully equipped to extract the ultraviolet divergences, first from the diagrams with a fermionic closed loop, and subsequently from diagrams with external fermion lines. Fortunately, some of the diagrams were already calculated in chapter 9 for the abelian case and the results were listed in (9.31-9.33). For these diagrams only minor changes are required and the result can be written down without much work.

(a) *Vacuum polarization diagram*

This diagram is the same as the diagram calculated in chapter 9 except that the coupling of the gauge field to the fermions is not equal to  $-ie\gamma_\mu$ , but to  $gt_a\gamma_\mu$ . Therefore in the expression for the vacuum polarization diagram (cf. 9.31) a factor  $-e^2$  is to be replaced by  $g^2 \text{Tr}(t_a t_b)$ . Furthermore there will

be a factor  $N_f$  because we have to sum over the contributions of the various fermion multiplets. Hence we obtain

$$\Pi_{\mu\nu}^{ab}(k^2) = -N_f C_2(R) \frac{\dim R}{\dim G} \frac{g^2 \mu^\epsilon}{6\pi^2} \frac{1}{\epsilon} \delta^{ab} (k^2 \eta_{\mu\nu} - k_\mu k_\nu). \quad (14.24)$$

The divergent term is cancelled by the contribution of the first term in the counterterm Lagrangian (14.14).

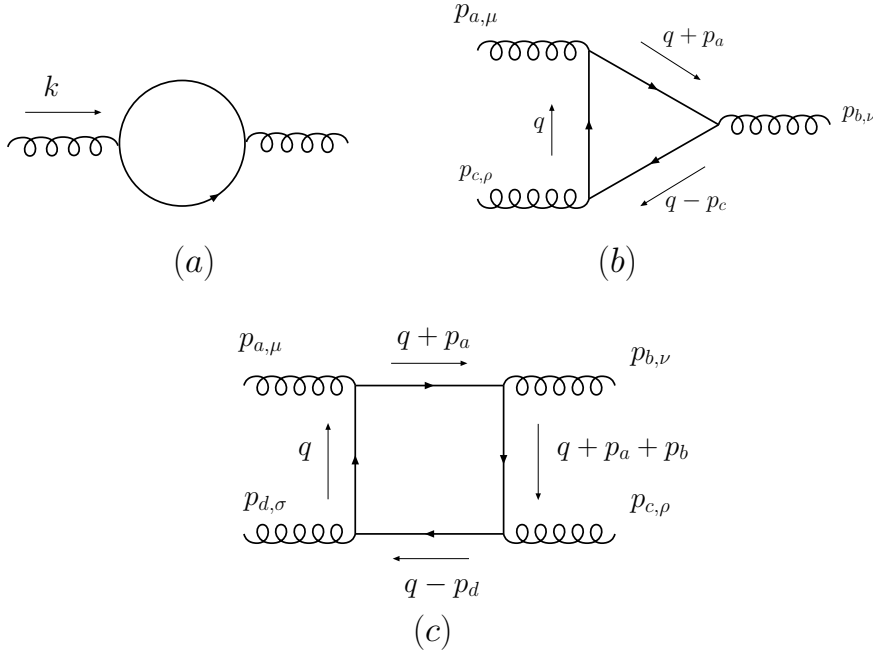


Figure 14.1: The divergent diagrams with one closed fermion loop: the vacuum polarization diagram (a), the triangle diagram (b) and the box diagram (c).

(b) *Triangle diagrams*

As shown in fig 14.1 there is a divergent diagram with three gauge fields attached to the fermion loop. At first sight one may think that this diagram will also appear in the abelian theory. Strictly speaking this is indeed so, but one should be aware of the fact that there are in fact two different diagrams, depending on the order in which the gauge-field lines have been attached to the fermion line. In the abelian case these two diagrams cancel exactly (at least for pure vector coupling). This is a consequence of charge-conjugation invariance: according to Furry's theorem fermion loops with an odd number of abelian gauge fields attached in all possible ways cancel (see problem 8.1).

Let us now consider the triangle graph with three gauge fields carrying group indices  $a, b, c$ , polarization indices  $\mu, \nu, \rho$  and incoming momenta  $p^a, p^b, p^c$ , respectively; they are attached in this order to a closed fermion line (when following the orientation of the fermion line). The expression corresponding to this diagram is

$$T_{\mu\nu\rho}^{abc}(p^a, p^b, p^c) = -N_f g^3 \text{Tr}(t_c t_b t_a) \int \frac{d^n q}{i(2\pi)^n} \times \frac{\text{Tr} [(-i \not{q} + m) \gamma_\rho (-i(\not{q} - \not{p}^c) + m) \gamma_\nu (-i(\not{q} + \not{p}^a) + m) \gamma_\mu]}{(q^2 + m^2)((q - p^c)^2 + m^2)((q + p^a)^2 + m^2)}. \quad (14.25)$$

Note that we have included a minus sign for the closed fermion loop and divided by a factor  $i(2\pi)^n$  in order to compare to the lowest-order vertex (cf. 9.29).

The divergent terms in (14.25) come from the terms in the numerator proportional to  $q^3$  or  $q^2$ . The term proportional to  $m q^2$  is proportional to the trace over an odd number of gamma matrices, which vanishes. Hence the relevant part of the trace in the numerator is

$$i \text{Tr} [\not{q} \gamma_\rho \not{q} \gamma_\nu \not{q} \gamma_\mu - \not{p}^c \gamma_\nu \not{q} \gamma_\mu \not{q} \gamma_\rho + \not{p}^a \gamma_\mu \not{q} \gamma_\rho \not{q} \gamma_\nu]. \quad (14.26)$$

At this point one may use the expressions for the divergent integrals (14.21) and (14.22) and then evaluate the spinor trace. However, we find it more convenient to first perform the trace and then use the expressions for the integrals; here the reader should realize that the trace can be directly evaluated in  $n = 4$  dimensions, as we are only interested in the residue of the  $1/\epsilon$  pole term. Before evaluating the trace, we may use the relation

$$\not{q} \gamma_\mu \not{q} = -q^2 \gamma_\mu + 2q_\mu \not{q} \quad (14.27)$$

to reduce the number of gamma matrices inside the trace. One is then left with a trace over four or two gamma matrices, which is easily computed (cf. appendix E.4 or 9.4). A few lines of calculation show that (14.26) is equal to

$$4i \left\{ \eta_{\mu\nu} [q^2(p^a + p^c - q)_\rho - 2q \cdot p^a q_\rho] + \eta_{\nu\rho} [-q^2(p^a + p^c + q)_\mu + 2q \cdot p^c q_\mu] + \eta_{\rho\mu} [q^2(-p^a + p^c - q)_\nu + 4q_\mu q_\nu q_\rho + 2q_\mu q_\rho (p^a - p^c)_\nu - 2q_\mu q_\nu p_\rho^c + 2q_\nu q_\rho p_\mu^a] \right\}. \quad (14.28)$$

Using the expressions for the divergent integrals (14.19- 14.22), this leads to

$$T_{\mu\nu\rho}^{abc}(p^a, p^b, p^c) = -iN_f \text{Tr}(t_c t_b t_a) \frac{\mu^\epsilon g^3}{6\pi^2} \frac{1}{\epsilon} \\ \times \left\{ \eta_{\mu\nu}(p^c + 2p^a)_\rho - \eta_{\nu\rho}(p^a + 2p^c)_\mu - \eta_{\rho\mu}(p^a - p^c)_\nu \right\}. \quad (14.29)$$

By virtue of momentum conservation,  $p^a + p^b + p^c = 0$ , the last factor can be written in a more symmetric form:  $-\{\eta_{\mu\nu}(p^b - p^a)_\rho + \eta_{\nu\rho}(p^c - p^b)_\mu + \eta_{\rho\mu}(p^a - p^c)_\nu\}$ . When combining the two possible diagrams, corresponding to inequivalent attachments of the gauge fields to the fermion loop, this term remains as an overall factor while there will be an additional term in the trace, which becomes  $\text{Tr}(t_c t_b t_a - t_b t_c t_a)$ . Using (14.27) we then obtain the following result for the divergent gauge-field coupling induced by a fermion loop,

$$\sum_{\text{diagrams}} T_{\mu\nu\rho}^{abc}(p^a, p^b, p^c) = iN_f C_2(R) \frac{\dim R}{\dim G} f_{abc} \frac{\mu^\epsilon g^3}{6\pi^2} \frac{1}{\epsilon} \\ \times \left\{ \eta_{\mu\nu}(p^b - p^a)_\rho + \eta_{\nu\rho}(p^c - p^b)_\mu + \eta_{\rho\mu}(p^a - p^c)_\nu \right\}. \quad (14.30)$$

Clearly, for an abelian theory this result vanishes in accord with Furry's theorem. Note that the infinite part is proportional to the lowest-order cubic gauge-field coupling, which is an obvious requirement for a renormalizable theory. This infinite term is cancelled by the contribution from the second term in the counterterm Lagrangian (14.14).

(c) *Box diagrams*

The box diagrams of a closed fermion line with four gauge fields attached with indices  $\mu, \nu, \rho, \sigma$  and  $a, b, c, d$ , respectively, in an order that coincides with the orientation of the fermion line, corresponds to the expression

$$B_{\mu\nu\rho\sigma}^{abcd}(p^a, p^b, p^c, p^d) = -N_f g^4 \text{Tr}(t_d t_c t_b t_a) \int \frac{d^n q}{i(2\pi)^n} \\ \times \frac{\text{Tr}[(\not{q} - im)\gamma_\sigma(\not{q} - \not{p}^d - im)\gamma_\rho(\not{q} + \not{p}^a + \not{p}^b - im)\gamma_\nu(\not{q} + \not{p}^a - im)\gamma_\mu]}{(q^2 + m^2)((q - p^d)^2 + m^2)((q + p^a + p^b)^2 + m^2)((q + p^a)^2 + m^2)}. \quad (14.31)$$

Again we included a minus sign for the closed fermion loop and a factor  $N_f$  for the sum over fermion representations, and we divided by the usual factor  $i(2\pi)^4$ .

The divergent terms originate from the  $q^4$  terms in the numerator so that the relevant part of the trace is

$$\text{Tr}[\not{q}\gamma_\sigma\not{q}\gamma_\rho\not{q}\gamma_\nu\not{q}\gamma_\mu]. \quad (14.32)$$

Also the external momenta in the denominator may be suppressed when calculating the divergent terms. Using again (14.27) to reduce the number of gamma matrices we find,

$$4 \left\{ q^4 [\eta_{\mu\nu} \eta_{\rho\sigma} + \eta_{\mu\sigma} \eta_{\nu\rho} - \eta_{\mu\rho} \eta_{\nu\sigma}] - 2q^2 [\eta_{\mu\nu} q_\rho q_\sigma + \eta_{\mu\sigma} q_\nu q_\rho + \eta_{\nu\rho} q_\mu q_\sigma + \eta_{\rho\sigma} q_\mu q_\nu] + 8q_\mu q_\nu q_\rho q_\sigma \right\}. \quad (14.33)$$

Substituting the results for the divergent integrals (14.19 - 14.23) this leads to

$$B_{\mu\nu\rho\sigma}^{abcd}(p^a, p^b, p^c, p^d) = N_f \frac{\mu^\epsilon g^4}{6\pi^2} \frac{1}{\epsilon} \text{Tr}(t_d t_c t_b t_a) \left\{ \eta_{\mu\nu} \eta_{\rho\sigma} + \eta_{\mu\sigma} \eta_{\nu\rho} - 2\eta_{\mu\rho} \eta_{\nu\sigma} \right\}. \quad (14.34)$$

This result must now be combined with that of five other diagrams where the gauge fields have been attached in an inequivalent order to the fermion loop. As the external momenta have been suppressed, this amounts to taking the linear combination

$$B_{\mu\nu\rho\sigma}^{abcd} + B_{\mu\nu\sigma\rho}^{abcd} + B_{\mu\rho\nu\sigma}^{abcd} + B_{\mu\rho\sigma\nu}^{abcd} + B_{\mu\sigma\rho\nu}^{abcd} + B_{\mu\sigma\nu\rho}^{abcd}. \quad (14.35)$$

The result then becomes proportional to traces of products of two commutators. Summing all contributions and using the last result in (14.8) yields

$$\begin{aligned} \sum_{\text{diagrams}} B_{\mu\nu\rho\sigma}^{abcd}(p^a, p^b, p^c, p^d) &= N_f C_2(R) \frac{\dim R}{\dim G} \frac{\mu^\epsilon g^4}{6\pi^2} \frac{1}{\epsilon} \\ &\times \left\{ \eta_{\mu\nu} \eta_{\rho\sigma} (f_{ace} f_{bde} + f_{ade} f_{bce}) + \eta_{\mu\sigma} \eta_{\nu\rho} (f_{abe} f_{dce} + f_{ace} f_{dbe}) \right. \\ &\quad \left. + \eta_{\mu\rho} \eta_{\nu\sigma} (f_{abe} f_{cde} + f_{ade} f_{cbe}) \right\}. \quad (14.36) \end{aligned}$$

Clearly this result vanishes for abelian theories, as we know from quantum electrodynamics (cf. problem 9.2). The above ultraviolet divergence is just proportional to the lowest-order quartic gauge-field vertex, which makes it consistent with renormalizability. It cancels against the contribution from the last term in the counterterm Lagrangian (14.14). (9.32)

(d) *Self-energy diagrams*

These diagrams are the same as the diagram calculated in chapter 9, except that the gauge field couples to the vertex with a factor  $g t_a \gamma_\mu$  rather than with  $-ie\gamma_\mu$ ; furthermore one must sum over the contributions of the various

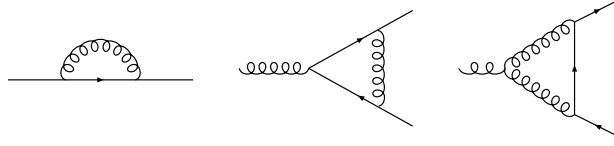


Figure 14.2: The divergent diagrams with external fermion lines: the self-energy diagram (d) and the vertex diagrams (e.1) and (e.2)

gauge fields. Consequently the factor  $e^2$  must be replaced by  $C_2(R)$  times the unit matrix (cf. 14.3). From comparison with the results quoted in (9.32) we thus obtain straightforwardly

$$\Sigma(p) = -C_2(R) \frac{g^2 \mu^\epsilon}{8\pi^2} \frac{1}{\epsilon} (m(3 + \lambda^{-2}) + i\not{p}\lambda^{-2}), \quad (14.37)$$

for each fermion. Observe that we do not indicate the group-representation indices of the fermions; (14.37) is thus proportional to the identity matrix in the corresponding space. The divergence is precisely cancelled by the contribution from the first term in the counterterm Lagrangian (14.15).

(e) *Vertex diagrams with external fermions*

There are two types of diagrams, indicated by (e.1) and (e.2) in fig 14.2. The first one is known from quantum electrodynamics and was already calculated in chapter 9. We take the result as quoted in (8.36) after replacing  $ie^3$  by  $g^3 t_b t_a t_b$ ,

$$\left[ \Lambda_\mu^a(p', p) \right]_{(1)} = -(C_2(R) - \frac{1}{2}C_2(G)) \lambda^{-2} \frac{g^3 \mu^\epsilon}{8\pi^2} \frac{1}{\epsilon} \gamma_\mu t_a, \quad (14.38)$$

where we used the second line of (14.8).

The second graph (e.2) is not present for the abelian theory and involves the cubic gauge-field vertex. Before writing down the corresponding expression, let us first consider a useful intermediate result, which will also be convenient for the calculations in subsequent sections. Consider a cubic gauge-field vertex, where a gauge field with incoming momentum  $Q$  and indices  $\mu, a$  couples to two gauge fields with incoming momenta  $q - \frac{1}{2}Q$  and  $-q - \frac{1}{2}Q$ , and indices  $\nu, b$  and  $\rho, c$ , respectively. To each of the latter two gauge fields we have connected a propagator (cf. fig 14.3). The expression corresponding to this diagram will be written as (we ignore factors  $i(2\pi)^4$ )

$$ig f_{abc} \frac{1}{(q - \frac{1}{2}Q)^2 (q + \frac{1}{2}Q)^2} V_{\mu\nu\rho}(Q, q - \frac{1}{2}Q, -q - \frac{1}{2}Q), \quad (14.39)$$

where

$$\begin{aligned}
V_{\mu\nu\rho}(Q, q - \tfrac{1}{2}Q, -q - \tfrac{1}{2}Q) &= \eta_{\mu\rho}(q + \tfrac{3}{2}Q)_\nu + \eta_{\mu\nu}(q - \tfrac{3}{2}Q)_\rho - 2\eta_{\nu\rho}q_\mu \\
&- \frac{(1 - \lambda^{-2})(q - \tfrac{1}{2}Q)_\nu}{(q - \tfrac{1}{2}Q)^2} \left[ \eta_{\mu\rho}((q + \tfrac{1}{2}Q)^2 - Q^2) - \right. \\
&\quad \left. (q + \tfrac{1}{2}Q)_\mu(q + \tfrac{1}{2}Q)_\rho + Q_\mu Q_\rho \right] \\
&- \frac{(1 - \lambda^{-2})(q + \tfrac{1}{2}Q)_\rho}{(q + \tfrac{1}{2}Q)^2} \left[ \eta_{\mu\nu}((q - \tfrac{1}{2}Q)^2 - Q^2) - \right. \\
&\quad \left. (q - \tfrac{1}{2}Q)_\mu(q - \tfrac{1}{2}Q)_\nu + Q_\mu Q_\nu \right] \\
&- \frac{(1 - \lambda^{-2})^2(q - \tfrac{1}{2}Q)_\nu(q + \tfrac{1}{2}Q)_\rho}{(q - \tfrac{1}{2}Q)^2(q + \tfrac{1}{2}Q)^2} \left[ q_\mu Q^2 - Q_\mu q \cdot Q \right].
\end{aligned}$$

It is now relatively easy to write down the expression for the vertex diagram (e.2),

$$\begin{aligned}
\left[ \Lambda_\mu^a(p', p) \right]_{(2)} &= \\
ig^3 \int \frac{d^n q}{i(2\pi)^n} \frac{f_{abc} t_b t_c \gamma^\nu (-i\not{q} - \tfrac{1}{2}i(\not{p}' + \not{p}) + m)\gamma^\rho}{((q + \tfrac{1}{2}(p + p'))^2 + m^2)(q - \tfrac{1}{2}Q)^2(q + \tfrac{1}{2}Q)^2} \\
&\quad \times V_{\mu\nu\rho}(Q, q - \tfrac{1}{2}Q, -q - \tfrac{1}{2}Q) \quad (14.40)
\end{aligned}$$

where  $Q = p' - p$  is the incoming gauge-field momentum and  $p$  and  $p'$  are the momenta of the incoming and outgoing fermion, respectively. The gauge-group factor can be rewritten using the first result in (14.8). As the integral is only logarithmically divergent, one can ignore the external momenta in the numerator. This yields

$$\begin{aligned}
\left[ \Lambda_\mu^a(p', p) \right]_{(2)} &= \\
\frac{1}{2}g^3 C_2(G) t_a \int \frac{d^n q}{i(2\pi)^n} \frac{\gamma^\nu \not{q} \gamma^\rho}{((q + \tfrac{1}{2}(p + p'))^2 + m^2)(q - \tfrac{1}{2}Q)^2(q + \tfrac{1}{2}Q)^2} \\
&\times \left\{ \eta_{\mu\rho}q_\nu + \eta_{\mu\nu}q_\rho - 2\eta_{\nu\rho}q_\mu - (1 - \lambda^{-2}) \left[ \frac{\eta_{\mu\rho}q_\nu q^2 - q_\mu q_\nu q_\rho}{(q - \tfrac{1}{2}Q)^2} \right. \right. \\
&\quad \left. \left. + \frac{\eta_{\mu\nu}q_\rho q^2 - q_\mu q_\nu q_\rho}{(q + \tfrac{1}{2}Q)^2} \right] \right\} + \text{finite terms}, \quad (14.41)
\end{aligned}$$

where we used again (14.8); the terms proportional to  $(1 - \lambda^{-2})^2$  were suppressed as they give rise to finite contributions. Writing out the various terms

in the above expressions, changing  $q^2$  terms in the denominator by  $(q \pm \frac{1}{2}Q)^2$ , whenever possible, to cancel them against similar factors in the denominator, one is left with integrals of the type discussed before. A straightforward evaluation then shows that

$$\left[ \Lambda_\mu^a(p', p) \right]_{(2)} = -\frac{3}{4}C_2(G) (1 + \lambda^{-2}) \frac{g^3 \mu^\epsilon}{8\pi^2} \frac{1}{\epsilon} \gamma_\mu t_a. \quad (14.42)$$

The combined contribution to the fermion vertex diagram is thus

$$\Lambda_\mu^a(p', p) = -\left\{ C_2(R) \lambda^{-2} + \frac{1}{4}C_2(G) (3 + \lambda^{-2}) \right\} \frac{g^3 \mu^\epsilon}{8\pi^2} \frac{1}{\epsilon} \gamma_\mu t_a. \quad (14.43)$$

This divergence is cancelled by the contribution from the second term in the counterterm Lagrangian (14.15).

We should point out that there is a subtlety with the vertex diagrams. As we already discussed extensively in chapter 8, these diagrams are also infrared divergent. Those divergences only manifest themselves when the fermion momenta approach the mass shell and the momentum transfer  $Q^2$  tends to zero. Hence one must be careful in taking certain limits when extracting the ultraviolet divergent terms and not drop the dependence on the external momenta in the propagators too early. In the expressions derived for the divergent integrals (cf. 14.19 - 14.23) this problem does not arise when the masses in the denominators are nonvanishing. Nevertheless, we may still apply these expressions for zero mass, as long as we avoid putting the external lines on shell. These subtleties are important in quantum chromodynamics. In the next section we will discuss the infrared divergences in a little more detail.

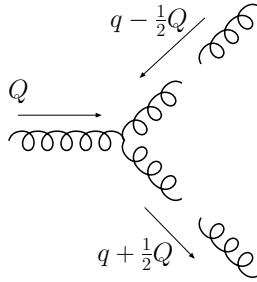


Figure 14.3: A cubic gauge-field vertex with two propagators attached, as described in the text.

#### 14.4. Vacuum polarization; ultraviolet versus infrared divergences

The evaluation of the one-loop graphs for the pure gauge theory, which consists only of gauge and ghost fields, is considerably more complicated than that of the diagrams considered in the previous section. Nevertheless, in order to establish the renormalization of the theory at the one-loop level, it is necessary to compute them all. This will give us ample opportunity to exhibit all the intricacies of diagrams that involve gauge fields.

In principle we will be interested in the ultraviolet divergences. However, in this section we present a detailed treatment of the full one-loop vacuum polarization for the gauge fields, in order to exhibit the subtleties that one encounters in diagrams that are both ultraviolet and infrared divergent. The presence of the latter is caused by the fact that gauge and ghost fields are massless (at least in covariant gauges without spontaneous symmetry breaking). The relative simplicity of the vacuum-polarization diagrams is such that we can explicitly demonstrate their most salient features. Some of this material will again be relevant in the next chapter on perturbative quantum chromodynamics. In the following section we turn to the diagrams with three or four external gauge or ghost fields. There we restrict ourselves to the ultraviolet divergent part, without paying attention to infrared divergent or finite parts.

The diagrams that contribute to the vacuum polarization are of three kinds, as is shown in Fig. 14.4. We first concentrate on diagram (a.1), which involves two three-point indices for the gauge fields. The Feynman rules given in section 13.5 yield the following expression

$$\begin{aligned} \left[ \Pi_{\mu\nu}^{ab}(k) \right]_{(1)} &= \frac{1}{2} g^2 f_{acd} f_{bcd} \int \frac{d^n q}{i(2\pi)^n} \frac{1}{(q - \frac{1}{2}k)^2 (q + \frac{1}{2}k)^2} \left[ \eta_{\mu\sigma} (-q - \frac{3}{2}k)_\rho \right. \\ &\quad \left. + \eta_{\mu\rho} (-q + \frac{3}{2}k)_\sigma + 2\eta_{\rho\sigma} q_\mu \right] V_\nu^{\rho\sigma}(k, q - \frac{1}{2}k, -q - \frac{1}{2}k), \quad (14.44) \end{aligned}$$

where here and elsewhere in this section we include the standard normalization factor  $[-i(2\pi)^4]^{-1}$  (cf. (2.64)). Here the indices  $c, d$  and  $\rho, \sigma$  refer to the internal gauge-field lines. Note the factor  $1/2$ , which is required to avoid overcounting of the diagrams, as all possible ways of connecting to the vertices are already included in the definition of the three-point vertex. Substituting the expression for  $V_\nu^{\rho\sigma}$ , a straightforward but somewhat lengthy calculation

gives

$$\begin{aligned}
 \left[ \Pi_{\mu\nu}^{ab}(k) \right]_{(1)} &= -\frac{1}{2}g^2 C_2(G) \delta_{ab} \int \frac{d^n q}{i(2\pi)^n} \frac{1}{(q - \frac{1}{2}k)^2 (q + \frac{1}{2}k)^2} \\
 &\times \left\{ \left( \frac{9}{2}k^2 + 2q^2 \right) \eta_{\mu\nu} + (4n - 6)q_\mu q_\nu - \frac{9}{2}k_\mu k_\nu - (1 - \lambda^{-2}) k_\mu k_\nu \right. \\
 &+ \frac{1 - \lambda^{-2}}{(q - \frac{1}{2}k)^2} \left[ - (k^2 - (q + \frac{1}{2}k)^2)^2 \eta_{\mu\nu} + ((q + \frac{1}{2}k)^2 - 2k^2) q_\mu q_\nu \right. \\
 &+ \left. \left. \left( (q + \frac{1}{2}k)^2 - \frac{1}{2}k^2 \right) (q_\mu k_\nu + k_\mu q_\nu) \right. \right. \\
 &\quad \left. \left. + \left( k^2 - \frac{5}{4}(q + \frac{1}{2}k)^2 \right) k_\mu k_\nu \right] \right. \\
 &+ \frac{1 - \lambda^{-2}}{(q + \frac{1}{2}k)^2} \left[ - (k^2 - (q - \frac{1}{2}k)^2)^2 \eta_{\mu\nu} + \left( (q - \frac{1}{2}k)^2 - 2k^2 \right) q_\mu q_\nu \right. \\
 &+ \left. \left. \left( (q - \frac{1}{2}k)^2 - \frac{1}{2}k^2 \right) (q_\mu k_\nu + k_\mu q_\nu) \right. \right. \\
 &\quad \left. \left. + \left( k^2 - \frac{5}{4}(q - \frac{1}{2}k)^2 \right) k_\mu k_\nu \right] \right. \\
 &+ \frac{(1 - \lambda^{-2})^2}{(q - \frac{1}{2}k)^2 (q + \frac{1}{2}k)^2} \left[ k^4 q_\mu q_\nu - k^2 q \cdot k (q_\mu k_\nu + k_\mu q_\nu) \right. \\
 &\quad \left. + (q \cdot k)^2 k_\mu k_\nu \right] \left. \right\}, \tag{14.45}
 \end{aligned}$$

To simplify this expression we first collect all terms with an explicit factor  $(q \pm \frac{1}{2}k)^2$  in the numerators, cancel them against similar terms in the denominator, and shift the integration momentum  $q$  to  $q \mp \frac{1}{2}k$ . We also bring the terms over a common denominator whenever necessary to make the denominators

symmetric under  $k \rightarrow -k$ . The result of this is

$$\begin{aligned}
\left[ \Pi_{\mu\nu}^{ab}(k) \right]_{(1)} = & \\
& - g^2 C_2(G) \delta_{ab} \int \frac{d^n q}{i(2\pi)^n} \frac{1}{(q - \frac{1}{2}k)^2 (q + \frac{1}{2}k)^2} \\
& \quad \times \left\{ \left( \frac{9}{4}k^2 + q^2 \right) \eta_{\mu\nu} + (2n - 3)q_\mu q_\nu - \frac{9}{4}k_\mu k_\nu - \frac{1}{2}(1 - \lambda^{-2}) k_\mu k_\nu \right\} \\
& - g^2 C_2(G) \delta_{ab} \int \frac{d^n q}{i(2\pi)^n} \frac{1}{(q - \frac{1}{2}k)^4 (q + \frac{1}{2}k)^4} \\
& \quad \times \left\{ (1 - \lambda^{-2}) k^2 \left[ -k^2 (q^2 + \frac{1}{4}k^2) \eta_{\mu\nu} - 2(q^2 + \frac{1}{4}k^2) q_\mu q_\nu \right. \right. \\
& \quad \quad \left. \left. - \frac{1}{2}q \cdot k (q_\mu k_\nu + k_\mu q_\nu) + (q^2 + \frac{1}{4}k^2) k_\mu k_\nu \right] \right. \\
& \quad \left. + \frac{1}{2}(1 - \lambda^{-2})^2 \left[ k^4 q_\mu q_\nu - k^2 q \cdot k (q_\mu k_\nu + k_\mu q_\nu) + (q \cdot k)^2 k_\mu k_\nu \right] \right\} \\
& - g^2 C_2(G) \delta_{ab} \int \frac{d^n q}{i(2\pi)^n} \frac{1 - \lambda^{-2}}{q^4} \left\{ (k^2 - q^2) \eta_{\mu\nu} + q_\mu q_\nu \right\}.
\end{aligned} \tag{14.46}$$

Before we further evaluate the above expression, let us turn to the other two

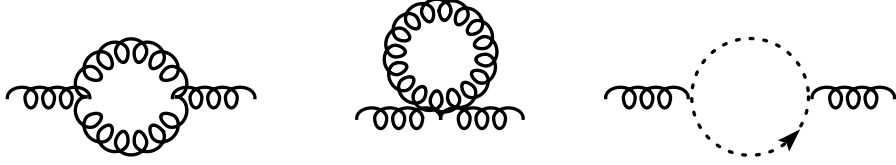


Figure 14.4: The vacuum polarization diagrams for the gauge fields.

diagrams (a.2) and (a.3). The diagrams (a.2) follow directly from the four-point vertex. Again, we divide by a factor 2 to avoid overcounting. The result reads

$$\begin{aligned}
\left[ \Pi_{\mu\nu}^{ab}(k) \right]_{(2)} = & \\
& g^2 f_{acd} f_{bcd} \int \frac{d^n q}{i(2\pi)^n} \left[ \eta_{\mu\nu} \eta_{\rho\sigma} - \eta_{\mu\rho} \eta_{\nu\sigma} \right] \frac{1}{q^2} \left[ \eta^{\rho\sigma} - (1 - \lambda^{-2}) \frac{q^\rho q^\sigma}{q^2} \right] \\
= & g^2 C_2(G) \delta_{ab} \int \frac{d^n q}{i(2\pi)^n} \left\{ \frac{n-1}{q^2} \eta_{\mu\nu} - \frac{1-\lambda^2}{q^4} (\eta_{\mu\nu} q^2 - q_\mu q_\nu) \right\},
\end{aligned} \tag{14.47}$$

The third diagram (a.3) gives rise to

$$\begin{aligned} \left[ \Pi_{\mu\nu}^{ab}(k) \right]_{(3)} &= -g^2 f_{acd} f_{bdc} \int \frac{d^n q}{i(2\pi)^n} \frac{(q + \frac{1}{2}k)_\mu (q - \frac{1}{2}k)_\nu}{(q - \frac{1}{2}k)^2 (q + \frac{1}{2}k)^2} \\ &= g^2 C_2(G) \delta_{ab} \int \frac{d^n q}{i(2\pi)^n} \frac{q_\mu q_\nu - \frac{1}{4}k_\mu k_\nu}{(q - \frac{1}{2}k)^2 (q + \frac{1}{2}k)^2} \end{aligned} \quad (14.48)$$

where we included a minus sign for the closed ghost loop and the proper normalization factor. In the last line we dropped the terms in the numerator that are odd in  $q$ .

Combining the expressions for the three diagrams gives

$$\begin{aligned} \Pi_{\mu\nu}^{ab}(k) &= -g^2 C_2(G) \delta_{ab} \int \frac{d^n q}{i(2\pi)^n} \frac{1}{(q - \frac{1}{2}k)^2 (q + \frac{1}{2}k)^2} \\ &\quad \times \left\{ (n-2) \left[ - (q^2 + \frac{1}{4}k^2) \eta_{\mu\nu} + 2q_\mu q_\nu \right] + 2(k^2 \eta_{\mu\nu} - k_\mu k_\nu) \right\} \\ &\quad - g^2 C_2(G) \delta_{ab} (1 - \lambda^{-2}) \int \frac{d^n q}{i(2\pi)^n} \frac{1}{(q - \frac{1}{2}k)^4 (q + \frac{1}{2}k)^4} \\ &\quad \times \left\{ -k^2 (2q^2 + k^2) q_\mu q_\nu + \left[ \frac{1}{2}(q^2 + \frac{1}{4}k^2)^2 + (k \cdot q)^2 \right] k^2 \eta_{\mu\nu} \right. \\ &\quad \quad \left. + \left[ \frac{1}{2}(q^2 + \frac{1}{4}k^2)^2 - k^2 (q^2 + \frac{1}{4}k^2) \right] (k^2 \eta_{\mu\nu} - k_\mu k_\nu) \right. \\ &\quad \quad \left. + \frac{1}{2} (2 - \lambda^{-2}) \left[ k^4 q_\mu q_\nu - k^2 q \cdot k (q_\mu k_\nu + k_\mu q_\nu) \right. \right. \\ &\quad \quad \left. \left. + (q \cdot k)^2 k_\mu k_\nu \right] \right\}. \end{aligned} \quad (14.49)$$

In order to extract a common denominator, we shifted the integration momentum in the terms proportional to  $q^{-2}$  and  $q^{-4}$  and multiplied numerators and denominators with the same factors.

For large  $q$  the integrand in the above expression behaves as  $q^{-2}$  and lower powers of  $q$ , so that we are dealing with quadratic, linear and logarithmic ultraviolet divergences. In addition there are infrared divergent contributions, associated with  $q = \pm \frac{1}{2}k$ . In principle we could ignore all this and just calculate the integral in  $n$  dimensions, encountering  $1/\epsilon$  pole terms associated with these divergences. However, in this way we would not be able to distinguish between ultraviolet and infrared divergences. This could be troublesome as the prescriptions for dealing with the two types of divergences are rather different. The ultraviolet divergences are removed by renormalization, as we explained in previous chapters. In contrast, infrared divergences are usually expected to vanish at the end of the calculation when computing physical results, such as cross sections. We demonstrated this already in section 4.6 and 9.6 in the context of quantum electrodynamics. Nevertheless the infrared divergences are encountered at an intermediate level, such as in the expression (14.49).

The first integral contains terms proportional to  $[(q + \frac{1}{2}k)^2(q - \frac{1}{2}k)^2]^{-1}$ , which generically give rise to a logarithmic divergence at  $k^2 = 0$ ; the second integral contains higher powers of  $(q \pm \frac{1}{2}k)^{-2}$ , which may give rise to infrared divergences that are independent of the value of  $k^2$ . All these divergences must be treated in a consistent fashion. This is notoriously difficult for nonabelian gauge theories. The simplest method is to introduce a small cut-off mass, as we did in chapter 9 for quantum electrodynamics. However, in that case the presence of the photon mass only causes minor violations of gauge invariance and does not affect the renormalizability of the theory. In the nonabelian gauge theories, where the gauge fields are self-interacting, the effect of the cut-off mass is much more severe. As mentioned above, dimensional regularization can also be employed for dealing with infrared divergences, but unlike for ultraviolet divergences the  $1/\epsilon$  poles are not cancelled at an intermediate level by some sort of renormalization scheme and one has to keep these terms until the end. If one knows that the quantity one is calculating is free of infrared divergences, then one could of course suppress all such divergences at intermediate levels of the calculation. There exists such a subtraction scheme, similar to minimal subtraction in the context of dimensional regularization, which can be used for this purpose. We will not discuss it here and refer the reader to the original literature.

Before proceeding we want to present some typical integrals. First we recall from section 9.3 that one can show by standard methods that

$$\int \frac{d^n q}{(q^2)^\alpha} = 0, \text{ unless } 2\alpha = n. \quad (14.50)$$

The question that arises is how to evaluate the integral over  $q^{-4}$ . Clearly this integral has both an ultraviolet as well as an infrared divergence. As the integrand behaves as  $q^{n-5}$  for large (Euclidean) momenta, analytic continuation to dimensions  $n > 4$  leads to an integral that is infrared but not ultraviolet finite, while continuation to  $n < 4$  makes the integral ultraviolet but not infrared finite. Consequently there is no region in the complex- $n$  plane for which the integral can be given a well-defined meaning. However, we can combine dimensional regularization with some other method to separate the divergences. For instance, let us insert a small mass  $\kappa$  and, by dimensional regularization, evaluate the integral

$$\int \frac{d^n q}{(q^2 + \kappa^2)^2} = -2i\pi^2 \left\{ \frac{1}{\epsilon} + \frac{1}{2}\gamma_E + \frac{1}{2} \ln \frac{\pi \kappa^2}{\mu^2} + O(\epsilon) \right\}, \quad (14.51)$$

which shows the ultraviolet divergence as a  $1/\epsilon$  pole and the infrared divergence as a  $\ln \kappa$  term. Alternatively we can introduce an ultraviolet regulariza-

tion depending on a large cut-off mass  $\Lambda$ ,

$$\int \frac{d^n q}{q^4} \frac{\Lambda^2}{q^2 + \Lambda^2} = 2 \int_0^1 dx \int d^n q \frac{x \Lambda^2}{(q^2 + \Lambda^2(1-x))^3}, \quad (14.52)$$

where we introduced Feynman parameters using (9.27). Performing the  $n$ -dimensional integral gives

$$i\pi^{2+\frac{1}{2}\epsilon} \Lambda^\epsilon \int_0^1 dx x (1-x)^{-1+\frac{1}{2}\epsilon}, \quad (14.53)$$

which can be evaluated by means of the standard formula for the Euler beta function

$$\int_0^1 dx x^\alpha (1-x)^\beta = \frac{\Gamma(\alpha+1)\Gamma(\beta+1)}{\Gamma(\alpha+\beta+2)} \equiv B(\alpha+1, \beta+1). \quad (14.54)$$

The result is

$$\int \frac{d^n q}{q^4} \frac{\Lambda^2}{q^2 + \Lambda^2} = 2i\pi^2 \left\{ \frac{1}{\epsilon} - \frac{1}{2} + \frac{1}{2}\gamma_E + \frac{1}{2} \ln \frac{\pi \Lambda^2}{\mu^2} + O(\epsilon) \right\}. \quad (14.55)$$

The  $1/\epsilon$  pole in (14.55) characterizes the infrared divergence and appears with opposite sign as compared to the ultraviolet pole in (14.51). Observe that the infrared pole emerges from the integration over the Feynman parameters. This is typical for infrared divergences.

When straightforwardly applying dimensional regularization, the  $1/\epsilon$  pole terms due to the ultraviolet and the infrared divergences cancel, and so do the finite remainders. However, when extracting the separate ultraviolet and infrared divergences one must remember to include these integrals appropriately, in spite of the fact that their combined result equals zero.

After this digression we continue the evaluation of the vacuum polarization, keeping track of what the precise nature is of the various divergences. It is not difficult to show the expression (14.49) is conserved, i.e. that it vanishes upon contraction with  $k^\mu$  and/or  $k^\nu$ . Here one uses that  $k \cdot q$  and  $q^2 + \frac{1}{4}k^2$  are proportional to the difference and the sum, respectively, of the two denominator factors. By partial fractioning the integrand and suitable changes in the integration momentum one proves the desired result. Alternatively, one can use (9.39) to evaluate the integrals with two uncontracted momenta in the numerator. Either way one concludes that (14.49) must take the form

$$\Pi_{\mu\nu}^{ab}(k) = g^2 C_2(G) \delta^{ab} \Pi(k^2) (k^2 \eta_{\mu\nu} - k_\mu k_\nu) \quad (14.56)$$

where  $\Pi(k^2)$  follows from taking the trace over  $\mu$  and  $\nu$  of both sides of the

equation and using (14.49),

$$\begin{aligned}
\Pi(k^2) = & \int \frac{d^n q}{i(2\pi)^n} \frac{1}{(q - \frac{1}{2}k)^2 (q + \frac{1}{2}k)^2} \left\{ \frac{(n-2)^2}{n-1} \frac{q^2 + \frac{1}{4}k^2}{k^2} - \frac{\frac{3}{2}n-1}{n-1} \right\} \\
& - \frac{1-\lambda^{-2}}{n-1} \int \frac{d^n q}{i(2\pi)^n} \frac{1}{(q - \frac{1}{2}k)^4 (q + \frac{1}{2}k)^4} \\
& \times \left\{ (n - \frac{5}{2})(q^2 + \frac{1}{4}k^2)^2 + \frac{1}{8}k^4 + n(q \cdot k)^2 - (n-1)k^2(q^2 + \frac{1}{4}k^2) \right. \\
& \left. + \frac{1}{2}(2 - \lambda^{-2})(k^2 q^2 - (q \cdot k)^2) \right\}.
\end{aligned} \tag{14.57}$$

We can further simplify this expression. The first term in the first line can be dropped, as it can be written as an integral over  $1/q^2$  (up to a term antisymmetric in  $q$ ) by shifting integration variables. Then in the first term of in the second integral  $(q^2 + \frac{1}{4}k^2)^2$  can be replaced by  $(q + \frac{1}{2}k)^2 (q - \frac{1}{2}k)^2 + (q \cdot k)^2$ . Finally, one observes that

$$\frac{n-4}{(q + \frac{1}{2}k)^2 (q - \frac{1}{2}k)^2} - \frac{2(q \cdot k)^2 - k^2(q^2 + \frac{1}{4}k^2)}{(q + \frac{1}{2}k)^4 (q - \frac{1}{2}k)^4}, \tag{14.58}$$

which itself does not give rise to infrared divergences associated with  $q = \pm \frac{1}{2}k$ , is a total divergence which can be dropped in the  $n$ -dimensional integral. Making use of this, we obtain the expression

$$\begin{aligned}
\Pi(k^2) = & \int \frac{d^n q}{i(2\pi)^n} \frac{1}{(q - \frac{1}{2}k)^2 (q + \frac{1}{2}k)^2} \\
& \times \frac{-2n^2 + 5n - 1 + \lambda^{-2}(2n^2 - 8n + 3)}{2(n-1)} \\
& + \frac{1-\lambda^{-2}}{2(n-1)} \int \frac{d^n q}{i(2\pi)^n} \frac{1}{(q - \frac{1}{2}k)^4 (q + \frac{1}{2}k)^4} \\
& \times \left\{ (q \cdot k)^2 - \frac{1}{4}k^4 - (2 - \lambda^{-2})(k^2 q^2 - (q \cdot k)^2) \right\}.
\end{aligned} \tag{14.59}$$

Only the first integral is ultraviolet divergent. The infrared divergences associated with  $q = \pm \frac{1}{2}k$  are absent in both integrals; in principle the terms proportional to  $(q \pm \frac{1}{2}k)^{-4}$  give rise to such divergences, but the numerator in the second integral of (14.59) vanishes for  $q = \pm \frac{1}{2}k$ , thus suppressing this singular behaviour. Only for  $k^2 = 0$  do we encounter infrared divergences in the form of  $\log k^2$  terms.

### 14.5. One-loop divergent graphs; gauge and ghost fields

After this explicit computation of the gauge-field vacuum polarization, we turn to an evaluation of the remaining one-loop divergences for the pure gauge theory. We try to follow the set-up of the previous subsection but concentrate as quickly as possible on the ultraviolet divergent terms. Therefore we drop contributions that are finite by power counting. First we give the result for the gauge-field vacuum polarization and then consider the diagrams with three and four external gauge fields. Finally we turn to the diagrams with external ghost lines, which are fortunately relatively easy to compute.

#### (a) Diagrams with two external gauge fields

These are the diagrams considered in section 14.4 (cf. fig. 14.4). We only have to extract the ultraviolet divergent part of (14.59), which equals

$$\Pi_{\mu\nu}^{ab}(k) = (13 - 3\lambda^{-2}) C_2(G) \delta^{ab} \frac{g^2 \mu^\epsilon}{48\pi^2 \epsilon} (k^2 \eta_{\mu\nu} - k_\mu k_\nu). \quad (14.60)$$

These divergences are cancelled by the contribution from the counterterm Lagrangian (14.16).

#### (b) Diagrams with three external gauge fields

The one-loop diagrams with three external gauge-field lines are shown in fig. 14.5. Let us start by giving the expressions corresponding to each of these graphs. The diagram (b.1) gives

$$\begin{aligned} \left[ T_{\mu\nu\rho}^{abc}(p^a, p^b, p^c) \right]_{(1)} &= -ig^3 f_{ade} f_{bdf} f_{cef} \\ &\times \int \frac{d^n q}{i(2\pi)^n} \frac{V_\mu^{\sigma\tau}(Q, q - \frac{1}{2}Q, -q - \frac{1}{2}Q)}{(q - \frac{1}{2}Q)^2 (q + \frac{1}{2}Q)^2 (q - \frac{1}{2}P)^2} \\ &\times \left\{ (-q - \frac{1}{2}Q + P)_\sigma \eta_{\nu\lambda} + (-q + Q - \frac{1}{2}P)_\lambda \eta_{\nu\sigma} \right. \\ &\quad \left. + (2q - \frac{1}{2}Q - \frac{1}{2}P)_\nu \eta_{\lambda\sigma} \right\} \\ &\times \left\{ (q - \frac{1}{2}Q - P)_\tau \eta_{\rho\lambda'} + (q + Q + \frac{1}{2}P)_{\lambda'} \eta_{\rho\tau} \right. \\ &\quad \left. + (-2q - \frac{1}{2}Q + \frac{1}{2}P)_\rho \eta_{\tau\lambda'} \right\} \\ &\times \left\{ \eta^{\lambda\lambda'} - (1 - \lambda^{-2}) \frac{(q - \frac{1}{2}P)^\lambda (q - \frac{1}{2}P)^{\lambda'}}{(q - \frac{1}{2}P)^2} \right\} \end{aligned} \quad (14.61)$$

where the momentum assignments are shown in the diagrams and  $Q = p^a$  and  $P = p^b - p^c$ . This diagram does not need any combinatorial factors. It contains

terms that are linearly and logarithmically divergent. Collecting terms in the integrand that behave asymptotically as  $q^{-3}$  or  $q^{-4}$  leads to the expression

$$\begin{aligned}
\left[ T_{\mu\nu\rho}^{abc}(p^a, p^b, p^c) \right]_{(1)} &= -\frac{1}{2} i g^3 C_2(G) f_{abc} \\
&\times \int \frac{d^n q}{i(2\pi)^n} \frac{1}{(q - \frac{1}{2}Q)^2 (q + \frac{1}{2}Q)^2 (q - \frac{1}{2}P)^2} \\
&\times \left\{ (4 - \lambda^{-2}) \left[ 6q_\mu q_\nu q_\rho - \frac{3}{2} q_\mu q_\nu (P - Q)_\rho - \frac{3}{2} q_\mu q_\rho (P + Q)_\nu \right] \right. \\
&\quad + \lambda^{-2} \left[ \eta_{\mu\nu} q_\rho q \cdot (P + Q) + \eta_{\mu\rho} q_\nu q \cdot (P - Q) + 2\eta_{\nu\rho} q_\mu q \cdot P \right] \\
&\quad \left. - \lambda^{-2} (q - \frac{1}{2}P)^2 \left[ \eta_{\mu\nu} (\frac{3}{2}P_\rho - \frac{7}{2}Q_\rho) + \eta_{\mu\rho} (\frac{3}{2}P_\nu + \frac{7}{2}Q_\nu) - 2\eta_{\nu\rho} P_\mu \right] \right\}
\end{aligned} \tag{14.62}$$

where we made use of (14.9). For the moment we leave the answer in this form, as we shall encounter similar expressions in diagram (b.3).

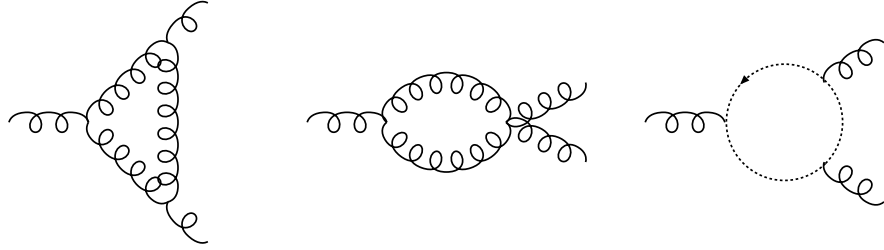


Figure 14.5: The diagrams with three external gauge fields.

The next diagram (b.2) requires a factor  $\frac{1}{2}$  to avoid overcounting, and has to be combined eventually with two similar expressions related to different attachments of the external lines. The expression is

$$\begin{aligned}
\left[ T_{\mu\nu\rho}^{abc}(p^a, p^b, p^c) \right]_{(2)} &= -\frac{1}{2} i g^3 f_{ade} (f_{bdf} f_{cef} + f_{bcf} f_{def}) \\
&\times \int \frac{d^n q}{i(2\pi)^n} \frac{1}{(q - \frac{1}{2}p^a)^2 (q + \frac{1}{2}p^a)^2} \\
&\times \left\{ V_{\mu\nu\rho}(p^a, q - \frac{1}{2}p^a, -q - \frac{1}{2}p^a) - V_{\mu\rho\nu}(p^a, q - \frac{1}{2}p^a, -q - \frac{1}{2}p^a) \right\}.
\end{aligned} \tag{14.63}$$

As we are interested in the ultraviolet contribution, we can suppress those terms in  $V_{\mu\nu\rho}$  that behave as  $1/q$ . The linearly divergent terms drop out,

either by antisymmetry in  $\nu$  and  $\rho$ , or by symmetric integration, and we are left with (using (14.4) and (14.9))

$$\begin{aligned} \left[ T_{\mu\nu\rho}^{abc}(p^a, p^b, p^c) \right]_{(2)} &= -\frac{3}{2}ig^3 C_2(G) f_{abc} \int \frac{d^n q}{i(2\pi)^n} \\ &\times \left\{ \frac{\frac{3}{2}(\eta_{\mu\rho} p_\nu^a - \eta_{\mu\nu} p_\rho^a)}{(q - \frac{1}{2}p^a)^2 (q + \frac{1}{2}p^a)^2} + \frac{(1 - \lambda^{-2}) q^2 q_\mu (q_\nu p_\rho^a - p_\nu^a q_\rho)}{(q - \frac{1}{2}p^a)^4 (q + \frac{1}{2}p^a)^4} \right\}. \end{aligned} \quad (14.64)$$

The other two graphs follow by interchanging  $\mu, a$  with  $\nu, b$  or  $\rho, c$ . As the integral is only logarithmically divergent we may suppress the external momenta in the denominator. One then easily combines the three graphs and obtains

$$\begin{aligned} \sum_{\text{diagrams}} \left[ T_{\mu\nu\rho}^{abc}(p^a, p^b, p^c) \right]_{(2)} &= -\frac{3}{2}ig^3 C_2(G) f_{abc} \int \frac{d^n q}{i(2\pi)^n} \\ &\times \left\{ \frac{\frac{3}{2} \eta_{\mu\rho} (p^a - p^c)_\nu + \eta_{\mu\nu} (p^b - p^a)_\rho + \eta_{\nu\rho} (p^c - p^b)_\mu}{q^4} \right. \\ &\left. + (1 - \lambda^{-2}) \frac{q_\mu q_\nu (p^a - p^b)_\rho + q_\mu q_\rho (p^c - p^a)_\nu + q_\nu q_\rho (p^b - p^c)_\mu}{q^6} \right\}. \end{aligned} \quad (14.65)$$

Finally we have the diagram (b.3) with the ghost loop. The following expression corresponds to a particular attachment of external lines, namely the one where the external lines with group indices  $a, b, c$  are attached in this order to the ghost line, following its orientation.

$$\begin{aligned} \left[ T_{\mu\nu\rho}^{abc}(p^a, p^b, p^c) \right]_{(3)} &= -ig^3 f_{ade} f_{bfd} f_{cef} \int \frac{d^n q}{i(2\pi)^n} \\ &\frac{(-q + \frac{1}{2}Q)_\mu (-q - \frac{1}{2}P)_\nu (-q - \frac{1}{2}Q)_\rho}{(q - \frac{1}{2}Q)^2 (q + \frac{1}{2}Q)^2 (q + \frac{1}{2}P)^2} \end{aligned} \quad (14.66)$$

The expression for the second diagram corresponding to the alternative attachment of external lines follows from interchanging the momenta  $p^b$  and  $p^c$  (so that  $P \rightarrow -P$ ), as well as the indices  $\nu, b$  and  $\rho, c$ . To bring the resulting expression over the same denominator, one changes the integration momentum  $q \rightarrow -q$ . The combined result of the two diagrams is then

$$\begin{aligned} \sum_{\text{diagrams}} \left[ T_{\mu\nu\rho}^{abc}(p^a, p^b, p^c) \right]_{(3)} &= -\frac{1}{2}ig^3 C_2(G) f_{abc} \\ &\times \int \frac{d^n q}{i(2\pi)^n} \frac{-2q_\mu q_\nu q_\rho + \frac{1}{2}q_\mu q_\nu (P - Q)_\rho + \frac{1}{2}q_\mu q_\rho (P + Q)_\nu}{(q - \frac{1}{2}Q)^2 (q + \frac{1}{2}Q)^2 (q - \frac{1}{2}P)^2}, \end{aligned} \quad (14.67)$$

where we used (14.9). This expression is identical to the first line in (14.62), so it can readily be combined with the diagram (b.1).

We now use the formulae (14.23 - 14.23) to extract the ultraviolet divergence in (14.62), (14.65) and (14.67). The combined result for all the graphs of fig. 14.5 reads

$$T_{\mu\nu\rho}^{abc}(p^a, p^b, p^c) = ig^3 \lambda^{-2} C_2(G) f_{abc} \frac{\mu^\epsilon}{96\pi^2} \frac{1}{\epsilon} \\ \times \{ (p^a - p^c)_\nu \eta_{\mu\rho} + (p^b - p^a)_\rho \eta_{\mu\nu} + (p^c - p^b)_\mu \eta_{\rho\nu} \}. \quad (14.68)$$

This divergence is cancelled by the second term in the counterterm Lagrangian (14.16).

(c) *Diagrams with four external gauge fields*

There are four types of one-loop diagrams with four external gauge fields. These diagrams are logarithmically divergent and their divergent part can be extracted conveniently by setting all external momenta to zero. As mentioned previously, the integrals are also infrared divergent, but using the results (14.23 - 14.23) for the divergent integrals, one correctly extracts the ultraviolet divergences.

With zero external momenta the expressions corresponding to the various graphs become relatively simple. Let us start with the first diagram of fig. 14.6,

$$\left[ B_{\mu\nu\rho\sigma}^{abcd}(0, 0, 0, 0) \right]_{(1)} = \\ g^4 f_{aef} f_{bge} f_{chg} f_{dfh} \int \frac{d^n q}{i(2\pi)^n} \frac{1}{q^8} V_\mu^{\lambda\tau}(0, q, -q) V_\rho^{\tau'\lambda'}(0, q, -q) \quad (14.69) \\ \times [q_{\lambda'} \eta_{\nu\lambda} + q_\lambda \eta_{\nu\lambda'} - 2q_\nu \eta_{\lambda\lambda'}] [q_\tau \eta_{\sigma\tau'} + q_{\tau'} \eta_{\sigma\tau} - 2q_\sigma \eta_{\tau\tau'}].$$

To this result we must add two similar expressions corresponding to diagrams with inequivalent attachments of external lines. No combinatoric factors are

required. Evaluating the expression under the integral one obtains

$$\begin{aligned}
\left[ B_{\mu\nu\rho\sigma}^{abcd}(0,0,0,0) \right]_{(1)} &= g^4 f_{aef} f_{bge} f_{chg} f_{dfh} \int \frac{d^n q}{i(2\pi)^n} \\
&\times \left\{ \lambda^{-4} \frac{\eta_{\mu\nu} \eta_{\rho\sigma} + \eta_{\mu\sigma} \eta_{\nu\rho}}{q^4} \right. \\
&+ \lambda^{-2} (4 - \lambda^{-2}) \frac{\eta_{\mu\nu} q_\rho q_\sigma + \eta_{\mu\sigma} q_\nu q_\rho + \eta_{\nu\rho} q_\mu q_\sigma + \eta_{\rho\sigma} q_\mu q_\nu}{q^6} \\
&\left. + (16(n-1) - 16\lambda^{-2} + 2\lambda^{-4}) \frac{q_\mu q_\nu q_\rho q_\sigma}{q^8} \right\} \quad (14.70) \\
&= -g^4 f_{aef} f_{bge} f_{chg} f_{dfh} \frac{\mu^\epsilon}{192 \pi^2} \frac{1}{\epsilon} \\
&\times \left\{ (48 + 32\lambda^{-2} \right. \\
&\quad \left. + 14\lambda^{-4})(\eta_{\mu\nu} \eta_{\rho\sigma} + \eta_{\mu\sigma} \eta_{\nu\rho}) + (48 - 16\lambda^{-2} + 2\lambda^{-4}) \eta_{\mu\rho} \eta_{\nu\sigma} \right\}.
\end{aligned}$$

The second diagram (c.2) does not require combinatorial factors either and

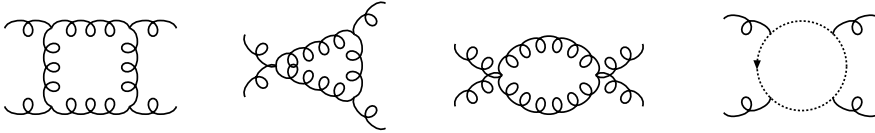


Figure 14.6: The diagrams with four external gauge fields.

has to be combined with five similar diagrams corresponding to inequivalent attachments of external lines.

$$\begin{aligned}
\left[ B_{\mu\nu\rho\sigma}^{abcd}(0,0,0,0) \right]_{(2)} &= g^4 f_{ahe} f_{beg} \int \frac{d^n q}{i(2\pi)^n} \frac{1}{q^6} V_{\mu}^{\tau\lambda}(0, q, -q) \\
&\times [q_\lambda \eta_{\nu\lambda'} + q_{\lambda'} \eta_{\nu\lambda} - 2q_\nu \eta_{\lambda\lambda'}] \left[ \eta^{\lambda'\tau'} - (1 - \lambda^{-2}) \frac{q^{\lambda'} q^{\tau'}}{q^2} \right] \\
&\times \left\{ \eta_{\rho\sigma} \eta_{\tau\tau'} (f_{gck} f_{hdk} + f_{gdk} f_{hck}) + \eta_{\sigma\tau'} \eta_{\tau\rho} (f_{ghk} f_{dck} + f_{gck} f_{dhk}) \right. \\
&\quad \left. + \eta_{\rho\tau'} \eta_{\sigma\tau} (f_{ghk} f_{cdk} + f_{gdk} f_{chk}) \right\}. \quad (14.71)
\end{aligned}$$

The product of the last line and the terms in front of the integral sign do not

involve the integration momentum  $q$ . They can be written as

$$\begin{aligned} & g^4 f_{ahe} f_{beg} (f_{gck} f_{hdk} + f_{gdk} f_{hck}) (\eta_{\rho\sigma} \eta_{\tau\tau'} - \frac{1}{2} \eta_{\rho\tau} \eta_{\sigma\tau'} - \frac{1}{2} \eta_{\rho\tau'} \eta_{\sigma\tau}) \\ & - g^4 f_{ahe} f_{beg} (f_{ghk} f_{cdk} + \frac{1}{2} f_{gck} f_{hdk} - \frac{1}{2} f_{gdk} f_{hck}) (\eta_{\rho\tau} \eta_{\sigma\tau'} - \eta_{\rho\tau'} \eta_{\sigma\tau}). \end{aligned} \quad (14.72)$$

It should be noted that the (anti)symmetry in  $\tau$  and  $\tau'$  is correlated with the (anti)symmetry in  $c$  and  $d$ . The factor in front of the second line can be simplified by using the Jacobi identity (13.2) and (14.9); it becomes equal to  $-\frac{3}{4}g^4 f_{abe} f_{cde} C_2(G)$ . Now we turn to the integrand, which contains the following combination of terms

$$\begin{aligned} & \int \frac{d^n q}{i(2\pi)^n} \left\{ - (4 - \lambda^{-2})(1 - \lambda^{-2}) \frac{q_\mu q_\nu q_\tau q_{\tau'}}{q^8} \right. \\ & \quad - \lambda^{-2} \frac{\eta_{\mu\tau} q_\nu q_{\tau'} + 2\eta_{\mu\tau'} q_\nu q_\tau + 2\eta_{\nu\tau} q_\mu q_{\tau'} + \eta_{\nu\tau'} q_\mu q_\tau}{q^6} \\ & \quad \left. + \lambda^{-4} \frac{\eta_{\mu\nu} q_\tau q_{\tau'}}{q^6} + 4 \frac{\eta_{\tau\tau'} q_\mu q_\nu}{q^6} + \lambda^{-2} \frac{\eta_{\mu\tau} \eta_{\nu\tau'}}{q^4} \right\} \\ & = -\frac{\mu^\epsilon}{192 \pi^2} \frac{1}{\epsilon} \left\{ (20 + 5\lambda^{-2} + 5\lambda^{-4}) \eta_{\mu\nu} \eta_{\tau\tau'} \right. \\ & \quad - (4 - 17\lambda^{-2} + \lambda^{-4}) \eta_{\mu\tau} \eta_{\nu\tau'} \\ & \quad \left. - (4 + 19\lambda^{-2} + \lambda^{-4}) \eta_{\mu\tau'} \eta_{\nu\tau} \right\}. \end{aligned} \quad (14.73)$$

Contracting (14.72) with (14.73) we obtain

$$\begin{aligned} & \left[ B_{\mu\nu\rho\sigma}^{abcd}(0, 0, 0, 0) \right]_{(2)} = -g^4 f_{ahe} f_{beg} (f_{gck} f_{hdk} + f_{gdk} f_{hck}) \\ & \quad \times \frac{\mu^\epsilon}{192 \pi^2} \frac{1}{\epsilon} (4 + \lambda^{-2} + \lambda^{-4}) (\eta_{\mu\rho} \eta_{\nu\sigma} + \eta_{\mu\sigma} \eta_{\nu\rho} + 13 \eta_{\mu\nu} \eta_{\rho\sigma}) \\ & \quad + 27\lambda^{-2} g^4 C_2(G) f_{abe} f_{cde} \frac{\mu^\epsilon}{192 \pi^2} \frac{1}{\epsilon} (\eta_{\mu\rho} \eta_{\nu\sigma} - \eta_{\mu\sigma} \eta_{\nu\rho}). \end{aligned} \quad (14.74)$$

For diagram (c.3) we first consider the product of the two vertices and contract over the group indices. For one vertex we take indices  $a\mu, b\nu$  for the external lines and indices  $f\mu', g\nu'$  for the internal lines; for the second vertex we choose indices  $c\rho, d\sigma$  for the external lines and indices  $f\rho', g\sigma'$  for the internal lines. Later we have to include two more graphs with inequivalent attachments of the external lines. The product of the two vertices and propagators then takes the following form

$$\begin{aligned} & \frac{1}{2} g^4 \left\{ f_{afe} f_{bge} (\eta_{\mu\nu} \eta_{\mu'\nu'} - \eta_{\mu\nu'} \eta_{\nu\mu'}) + f_{abe} f_{fge} \eta_{\mu\mu'} \eta_{\nu\nu'} \right. \\ & \quad \left. + [(a\mu) \leftrightarrow (b\nu)] \right\} \Delta^{\mu'\rho'} \Delta^{\nu'\sigma'} \\ & \quad \times \left\{ f_{cfe'} f_{dge'} (\eta_{\rho\sigma} \eta_{\rho'\sigma'} - \eta_{\rho\sigma'} \eta_{\sigma\rho'}) + f_{cde'} f_{fge'} \eta_{\rho\rho'} \eta_{\sigma\sigma'} \right. \\ & \quad \left. + [(c\rho) \leftrightarrow (d\sigma)] \right\}. \end{aligned} \quad (14.75)$$

The factor  $\frac{1}{2}$  was included to avoid overcounting. We note that each vertex consists of six different terms (cf. table 12.3), three of which can be obtained from the others by the interchange of the external-line indices. For the moment let us work out the terms that are given explicitly,

$$\begin{aligned}
& \left[ E_{\mu\nu\rho\sigma}^{abcd}(0,0,0,0) \right]_{(3)} = \\
& \frac{1}{2} g^4 f_{afe} f_{bge} f_{cfe'} f_{dge'} \int \frac{d^n q}{i(2\pi)^n} \left\{ \frac{\eta_{\mu\rho} \eta_{\nu\sigma}}{q^4} \right. \\
& + (n-3 + \lambda^{-4}) \frac{\eta_{\mu\nu} \eta_{\rho\sigma}}{q^4} - (1 - \lambda^{-2}) \frac{\eta_{\mu\rho} q_\nu q_\sigma + \eta_{\nu\sigma} q_\mu q_\rho}{q^6} \\
& + (1 - \lambda^{-4}) \frac{\eta_{\mu\nu} q_\rho q_\sigma + \eta_{\rho\sigma} q_\mu q_\nu}{q^6} + (1 - \lambda^{-2})^2 \frac{q_\mu q_\nu q_\rho q_\sigma}{q^8} \left. \right\} \\
& + \frac{1}{4} g^4 C_2(G) f_{abe} f_{cde} \int \frac{d^n q}{i(2\pi)^n} \left\{ \frac{2\eta_{\mu\nu} \eta_{\rho\sigma} - 2\eta_{\mu\sigma} \eta_{\nu\rho} + 2\eta_{\mu\rho} \eta_{\nu\sigma}}{q^4} \right. \\
& + 2(1 - \lambda^{-2}) \frac{\eta_{\mu\sigma} q_\nu q_\rho + \eta_{\nu\rho} q_\mu q_\sigma - \eta_{\mu\rho} q_\nu q_\sigma - \eta_{\nu\sigma} q_\mu q_\rho}{q^6} \\
& \left. - (1 - \lambda^{-4}) \frac{\eta_{\mu\nu} q_\rho q_\sigma + \eta_{\rho\sigma} q_\mu q_\nu}{q^6} \right\} \\
& + \text{three more terms} \\
& = -\frac{1}{2} g^4 f_{afe} f_{bge} f_{cfe'} f_{dge'} \frac{\mu^\epsilon}{192 \pi^2} \frac{1}{\epsilon} \\
& \times \left\{ (13 + 10\lambda^{-2} + \lambda^{-4}) \eta_{\mu\rho} \eta_{\nu\sigma} \right. \\
& \quad \left. + (1 - 2\lambda^{-2} + \lambda^{-4}) \eta_{\mu\sigma} \eta_{\nu\rho} + (37 - 2\lambda^{-2} + 13\lambda^{-4}) \eta_{\mu\nu} \eta_{\rho\sigma} \right\} \\
& - g^4 C_2(G) f_{abe} f_{cde} \frac{\mu^\epsilon}{64 \pi^2} \frac{1}{\epsilon} \\
& \times \left\{ 2(1 + \lambda^{-2})(\eta_{\mu\rho} \eta_{\nu\sigma} - \eta_{\mu\sigma} \eta_{\nu\rho}) + (3 + \lambda^{-4}) \eta_{\mu\nu} \eta_{\rho\sigma} \right\} \\
& + \text{three more terms.}
\end{aligned} \tag{14.76}$$

where the “three more terms” follow from the appropriate interchange of the indices. The factor  $C_2(G)$  arises from the use of (13.4) and (14.9).

Finally consider the diagram (c.4) with the ghost loop. It does not require a combinatorial factor and must be combined with five other diagrams corresponding to inequivalent attachments of the external lines. As the integral is only logarithmically divergent we may suppress the external momenta. The

corresponding expression is

$$\begin{aligned} \left[ B_{\mu\nu\rho\sigma}^{abcd}(0,0,0,0) \right]_{(4)} &= -g^4 f_{aeh} f_{bfe} f_{cgf} f_{dhg} \int \frac{d^n q}{i(2\pi)^n} \frac{q_\mu q_\nu q_\rho q_\sigma}{q^8} \\ &g^4 f_{aeh} f_{bfe} f_{cgf} f_{dhg} \frac{\mu^\epsilon}{192 \pi^2} \frac{1}{\epsilon} (\eta_{\mu\nu} \eta_{\rho\sigma} + \eta_{\mu\rho} \eta_{\nu\sigma} + \eta_{\mu\sigma} \eta_{\nu\rho}). \end{aligned} \quad (14.77)$$

It is relatively easy to combine the expressions for the four graphs (c.1-4). Rather than first combining the three or six graphs of each type corresponding to inequivalent attachments of the external lines, and then add all contributions, we note that the summation over different external-line attachments can be postponed until the end, where we then symmetrize over the index pairs  $(\mu, a)$ ,  $(\nu, b)$ ,  $(\rho, c)$  and  $(\sigma, d)$  of the external lines. There are twelve such permutations and we have to correct for that, as there were only three inequivalent attachments of external lines for the diagrams (c.1) and (c.3), and six for the diagrams (c.2) and (c.4). So we first multiply the expressions for the diagrams (c.1) and (c.3) by  $\frac{1}{4}$  and those for (c.2) and (c.4) by  $\frac{1}{2}$  and then add their contributions, after which we include all twelve permutations (because of the symmetry properties of the various graphs some of these twelve permutations will simply lead to identical results). According to this strategy the “three more terms” in (13.e18) can be counted as identical.

Let us now first add all terms proportional to the following product of four structure constants,  $f_{ahe} f_{bef} f_{cfg} f_{dgh}$ . By virtue of the antisymmetry of the structure constants this product is symmetric in  $a$  and  $c$  and in  $b$  and  $d$ . In some of the terms in (13.e16) and (13.e18) the indices are contracted differently, but those terms can yet be brought into the same form by interchanging the indices  $(\rho, c)$  and  $(\sigma, d)$  of the external lines. The result reads

$$\begin{aligned} g^4 f_{ahe} f_{bef} f_{cfg} f_{dgh} \frac{\mu^\epsilon}{192 \pi^2} \frac{1}{\epsilon} \left\{ (4 - 3\lambda^{-2})(\eta_{\mu\nu} \eta_{\rho\sigma} - \eta_{\mu\rho} \eta_{\nu\sigma}) \right. \\ \quad + (4 - 3\lambda^{-2})(\eta_{\mu\sigma} \eta_{\nu\rho} - \eta_{\mu\rho} \eta_{\nu\sigma}) \\ \quad \left. + (18 + 9\lambda^{-2} + 3\lambda^{-4})(\eta_{\mu\nu} \eta_{\rho\sigma} - \eta_{\mu\sigma} \eta_{\nu\rho}) \right\}. \end{aligned} \quad (14.78)$$

This expression must now be summed over all twelve permutations. However, the last term is antisymmetric in  $\nu$  and  $\rho$ , whereas the product of the structure constants is symmetric in the corresponding group indices  $b$  and  $c$ . Therefore this term cancels when summed over the corresponding index pairs. The two remaining combinations are antisymmetric in  $\nu\rho$  or in  $\rho\sigma$ . Therefore we can restrict ourselves to the part of product of the structure constants that is antisymmetric in  $bc$  or  $cd$ , respectively, so that the combined expression is

symmetric under the exchange of the corresponding external lines. These antisymmetric parts can be rewritten by means of the Jacobi identity (13.2), after which one uses (14.9) to write the (13.e20) as

$$g^4 C_2(G) \left(1 - \frac{3}{4}\lambda^{-2}\right) \frac{\mu^\epsilon}{192\pi^2} \frac{1}{\epsilon} \left\{ f_{ade} f_{bce} (\eta_{\mu\nu} \eta_{\rho\sigma} - \eta_{\mu\rho} \eta_{\nu\sigma}) \right. \\ \left. - f_{abe} f_{cde} (\eta_{\mu\sigma} \eta_{\nu\rho} - \eta_{\mu\rho} \eta_{\nu\sigma}) \right\}. \quad (14.79)$$

This expression can now be combined with the remaining contributions of the same structure in (13.e16), and (13.e18). After summing explicitly over the twelve permutations (so that for instance the last term proportional to  $(3 + \lambda^{-4})$  in (13.e18) cancels because it is antisymmetric in  $(\mu, a)$  and  $(\nu, b)$ ) one thus obtains

$$B_{\mu\nu\rho\sigma}^{abcd}(0, 0, 0, 0) = -g^4 (2 - 3\lambda^{-2}) \frac{\mu^\epsilon}{24\pi^2} \frac{1}{\epsilon} \\ \times \left\{ f_{ace} f_{bde} (\eta_{\mu\nu} \eta_{\rho\sigma} - \eta_{\mu\sigma} \eta_{\rho\nu}) + f_{ade} f_{bce} (\eta_{\mu\nu} \eta_{\sigma\rho} - \eta_{\mu\rho} \eta_{\sigma\nu}) \right. \\ \left. + f_{abe} f_{cde} (\eta_{\mu\rho} \eta_{\nu\sigma} - \eta_{\mu\sigma} \eta_{\nu\rho}) \right\}. \quad (14.80)$$

This divergence is cancelled by the contribution from the third term in the counterterm Lagrangian (13.b7).

(d) *Diagrams with external ghost fields*

The calculation of the divergent diagrams with external ghost lines resembles the calculations performed in the section 13.3 for diagrams with external fermion lines. As shown in Fig. 13.7, there is a self-energy diagram and two vertex diagrams. At first sight it seems that one can also have a box diagram with four external ghost lines, or a triangle diagram with two ghost ghost and two external gauge field lines. However, one of the momenta associated with the ghost vertices corresponds always to an external line, which reduces the large-momentum behaviour of the integrand. The expression for the ghost self-energy diagram equals

$$\Pi^{ab}(p) = g^2 \lambda^2 f_{cad} f_{cdb} \int \frac{d^n q}{i(2\pi)^n} \frac{p_\mu (p-q)_\nu}{i\lambda (p-q)^2 q^2} \left\{ \eta_{\mu\nu} - (1 - \lambda^{-2}) \frac{q_\mu q_\nu}{q^2} \right\}. \quad (14.81)$$

We now use the identity

$$\int \frac{d^n q}{i(2\pi)^n} \frac{q_\mu}{(p-q)^2 q^2} = \frac{1}{2} p_\mu \int \frac{d^n q}{i(2\pi)^n} \frac{1}{(p-q)^2 q^2}, \quad (14.82)$$

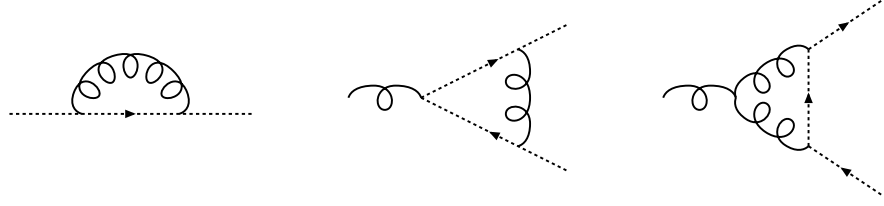


Figure 14.7: Diagrams with external ghost fields: self-energy (d.1), vertex (d.2) and vertex (d.3).

which follows from symmetric integration (cf. problem 13.x). Furthermore by partial fractioning, using  $2p \cdot q = -(p-q)^2 + q^2 + p^2$ , and dropping terms odd in  $q$ , we can extract a factor  $p^2$ , so that (13.e23) takes the form

$$\Pi^{ab}(p) = \frac{1}{4}i\lambda p^2 g^2 C_2(G) \delta^{ab} \int \frac{d^n q}{i(2\pi)^n} \frac{1}{(p-q)^2 q^2} \left\{ 3 - \lambda^{-2} - 2(1 - \lambda^{-2}) \frac{p \cdot q}{q^2} \right\}. \quad (14.83)$$

where we made use of (13.4). For  $p \neq 0$  the integral does not suffer from infrared divergences. The last term proportional to  $p \cdot q$  is also free of ultraviolet divergences. Hence the ultraviolet divergent term originates from the first few terms and we find

$$\Pi^{ab}(p) = -i\lambda(3 - \lambda^{-2}) g^2 C_2(G) \delta^{ab} p^2 \frac{\mu^\epsilon}{32\pi^2 \epsilon}. \quad (14.84)$$

This divergence is cancelled by the corresponding contribution from the counterterm Lagrangian (13.b8).

The expressions for the vertex diagrams (d.2) and (d.3) are ( $Q = p' - p$ )

$$\begin{aligned} \left[ \Lambda_{\mu;abc}(p', p) \right]_{(1)} &= -g^3 \lambda^3 f_{edc} f_{afd} f_{ebf} \\ &\quad \times \int \frac{d^n q}{i(2\pi)^n} \frac{(p-q)_\rho p'_\sigma (p'-q)_\mu}{(i\lambda)^2 (p-q)^2 (p'-q)^2 q^2} \left[ \eta^{\rho\sigma} - (1 - \lambda^{-2}) \frac{q^\rho q^\sigma}{q^2} \right], \\ \left[ \Lambda_{\mu;abc}(p', p) \right]_{(2)} &= ig^3 \lambda^2 f_{edc} f_{afd} f_{fbe} \\ &\quad \times \int \frac{d^n q}{i(2\pi)^n} \frac{p'_\rho (q + \frac{1}{2}(p+p'))^\sigma V_\mu^{\rho\sigma}(Q, q - \frac{1}{2}Q, -q - \frac{1}{2}Q)}{i\lambda (q + \frac{1}{2}(p+p'))^2 (q - \frac{1}{2}Q)^2 (q + \frac{1}{2}Q)^2}. \end{aligned} \quad (14.85)$$

Here we note that both diagrams are proportional to the external momenta associated with the outgoing ghost. The remaining integral is logarithmically

divergent, and its divergent part can be extracted by suppressing the external momenta in the integrand. Using also (14.9), the divergent part of the sum of the two graphs is equal to

$$\begin{aligned} \Lambda_{\mu,abc}(p', p) &= -\frac{1}{2}g^3\lambda^{-1} C_2(G) f_{abc} p'_\mu \int \frac{d^n q}{i(2\pi)^n} \frac{1}{q^4} \\ &= g^3\lambda^{-1} C_2(G) f_{abc} p'_\mu \frac{\mu^\epsilon}{16\pi^2} \frac{1}{\epsilon}, \end{aligned} \quad (14.86)$$

which is cancelled by the second term in the counterterm Lagrangian (13.b8).

### Problems

**14.1.** The generators of SU(N) in the defining  $N$ -dimensional representation consist of all independent  $N \times N$  traceless antihermitean matrices. Together with the identity matrix they form a complete basis for the general  $N \times N$  matrices. This implies that

$$\sum_{a=1}^{N^2-1} (t_a)_{ij} (t_a)_{kl} - (2N)^{-1} \delta_{ij} \delta_{kl} = -\frac{1}{2} \delta_{il} \delta_{jk}. \quad (1)$$

where we have used the normalization (14.5). Likewise, the generators of SO(N) in the defining representation form a complete basis of all  $N \times N$  antisymmetric matrices, which implies

$$\sum_{a=1}^{N(N-1)/2} (t_a)_{ij} (t_a)_{kl} = \frac{1}{4} (\delta_{ik} \delta_{jl} - \delta_{il} \delta_{jk}), \quad (2)$$

again with the same normalization (14.5). Prove these relations. Then apply them to  $\text{Tr}([t_a, t_b][t_a, t_b])$  and verify the result for  $C_2(G)$  as given in (14.7).

**14.2.** Consider a non-abelian gauge theory including, instead of fermions, scalar fields  $\phi_i$  with mass  $m$ , see also section 13.5. Omit any scalar self-interactions. Construct the counterterm Lagrangian in analogy to (14.13). Now study the self-energy corrections for the scalar propagator, and derive  $Z_\phi$  and  $Z_m$  to order  $g^2$ .

**14.3.** The differential and total cross sections for the reaction  $e^+ + e^- \rightarrow \mu^+ + \mu^-$ , when mediated by a single virtual photon, are given in (6.121) Use the gauge field Lagrangian (14.xx) to calculate the corresponding amplitude for the annihilation of a massless fermion with its antifermion producing a massive fermion-antifermion pair with mass  $m$ .

$$s^2 \frac{d^2\sigma}{dt_1 du_1} = \frac{g^4}{12\pi} \left[ \frac{t_1^2 + u_1^2}{s^2} + \frac{2m^2}{s} \right] \delta(s + t_1 + u_1),$$

and

$$\sigma = \frac{g^4}{54\pi s^2} (s + 2m^2) \beta.$$

We use the notation  $t_1 = t - m^2$ ,  $u_1 = u - m^2$  where  $s, t$  and  $u$  are defined in Table 6.9,  $\beta = (1 - 4m^2/s)^{1/2}$ . The results include a summation over final spins and gauge degrees of freedom for the fermion and an average over initial spins and gauge degrees of freedom.

**14.4.** Next consider the reaction where a photon and a quantum of the gauge field annihilate and produce a fermion antifermion pair of mass  $m$ . Use the same notation for the invariants as in the previous problem. Using the QED Lagrangian (5.41) and the gauge field Lagrangian (13.89), write down the two Feynman diagrams which contribute to the scattering amplitude and check that gauge invariance is satisfied. Calculate the differential cross section

$$s^2 \frac{d^2\sigma}{dt_1 du_1} = \alpha_{em} \frac{g^4}{16\pi} B_{QED} \delta(s + t_1 + u_1),$$

where

$$B_{QED} = \frac{t_1}{u_1} + \frac{u_1}{t_1} + \frac{4m^2 s}{t_1 u_1} \left(1 - \frac{m^2 s}{t_1 u_1}\right),$$

is the same factor that appears in the QED result (i.e., in the square of the amplitude for the reaction  $\gamma + \gamma \rightarrow \mu^+ + \mu^-$  which you can obtain by crossing from (9.126), setting  $k^2 = Q^2 = 0$  and dropping multiplicative factors). Note that we have summed over final spins and gauge degrees of freedom of the outgoing fermion-antifermion pair and averaged over the initial polarizations and gauge degrees of the incoming photon and gauge particle. Finally show that the total cross section is

$$\sigma = \frac{\alpha_{em} g^2}{2s} \left\{ \left(1 + \frac{4m^2}{s} - \frac{8m^4}{s^2}\right) \ln\left(\frac{1+\beta}{1-\beta}\right) - \left(1 + \frac{4m^2}{s}\right) \beta \right\}.$$

**14.5.** Now consider the reaction where two gauge field quanta annihilate into a massive fermion-antifermion pair. Use the same notation for the invariants as in the previous two problems and the Feynman rules for the gauge field Lagrangian (13.89). Write down the three Feynman diagrams which contribute to the scattering amplitude and check that gauge invariance is satisfied. Now drop terms in the amplitude which vanish upon contraction with the external polarization vectors. (Remember that we can always consider the Born amplitude as the imaginary part of a higher order amplitude and which would involve two gauge propagators and therefore Fadeev-Popov ghost contributions, so the sum over two external gauge field polarization vectors must be considered carefully). Derive the following results for the traces over the SU(3) matrices

$$T_1 = \text{Tr}(\lambda_a \lambda_b \lambda_b \lambda_a) = 2 \left( \frac{56}{3} + 24 \right),$$

and

$$T_2 = \text{Tr}(\lambda_a \lambda_b \lambda_a \lambda_b) = 2 \left( \frac{56}{3} - 24 \right).$$

where  $\lambda_a$  are the representation matrices satisfying the Lie algebra commutation relations. Split the traces of the Dirac matrices in the square of the amplitude into coefficients of  $T_1$  and  $T_2$ . Then calculate the two traces and show that their sum yields  $8B_{QED}$  where  $B_{QED}$  is the Abelian result found in the previous problem. Show that the difference of the two traces yields  $8(1 - 4t_1u_1/s^2)B_{QED}$ . Then add all the terms and show that the differential scattering amplitude takes the form

$$s^2 \frac{d^2\sigma}{dt_1 du_1} = \frac{g^4}{256\pi} \left\{ 3 \left( 1 - \frac{2t_1u_1}{s^2} \right) - \frac{1}{3} \right\} \left[ \frac{t_1}{u_1} + \frac{u_1}{t_1} + \frac{4m^2s}{t_1u_1} \left( 1 - \frac{m^2s}{t_1u_1} \right) \right] \delta(s+t_1+u_1),$$

Note that we have summed over final spins and colours and averaged over initial polarizations and colours. Finally show that the total cross section is

$$\sigma = \frac{g^4}{48\pi s} \left\{ \left( 1 + \frac{4m^2}{s} + \frac{m^4}{s^2} \right) \ln \left( \frac{1+\beta}{1-\beta} \right) - \left( 7 + \frac{31M^2}{s} \right) \frac{\beta}{4} \right\}.$$

For the corresponding calculations in the SU(3) gauge field theory usually referred to as Quantum Chromodynamics see; M. Glück, J.F. Owens and E. Reya, Phys. Rev. D17 (1978) 2324; B.L. Combridge, Nucl. Phys. B151 (1979) 429; J. Babcock, D. Sivers and S. Wolfram, Phys. Rev. D18 (1978) 162.